NBS TECHNICAL NOTE 1019

U.S. DEPARTMENT OF COMMERCE/National Bureau of Standards

Measurement of Optical Fiber Bandwidth in the Time Domain

NATIONAL BUREAU OF STANDARDS

The National Bureau of Standards[1] was established by an act of Congress on March 3, 1901. The Bureau's overall goal is to strengthen and advance the Nation's science and technology and facilitate their effective application for public benefit. To this end, the Bureau conducts research and provides: (1) a basis for the Nation's physical measurement system, (2) scientific and technological services for industry and government, (3) a technical basis for equity in trade, and (4) technical services to promote public safety. The Bureau's technical work is performed by the National Measurement Laboratory, the National Engineering Laboratory, and the Institute for Computer Sciences and Technology.

THE NATIONAL MEASUREMENT LABORATORY provides the national system of physical and chemical and materials measurement; coordinates the system with measurement systems of other nations and furnishes essential services leading to accurate and uniform physical and chemical measurement throughout the Nation's scientific community, industry, and commerce; conducts materials research leading to improved methods of measurement, standards, and data on the properties of materials needed by industry, commerce, educational institutions, and Government; provides advisory and research services to other Government agencies; develops, produces, and distributes Standard Reference Materials; and provides calibration services. The Laboratory consists of the following centers:

Absolute Physical Quantities[2] — Radiation Research — Thermodynamics and Molecular Science — Analytical Chemistry — Materials Science.

THE NATIONAL ENGINEERING LABORATORY provides technology and technical services to the public and private sectors to address national needs and to solve national problems; conducts research in engineering and applied science in support of these efforts; builds and maintains competence in the necessary disciplines required to carry out this research and technical service; develops engineering data and measurement capabilities; provides engineering measurement traceability services; develops test methods and proposes engineering standards and code changes; develops and proposes new engineering practices; and develops and improves mechanisms to transfer results of its research to the ultimate user. The Laboratory consists of the following centers:

Applied Mathematics — Electronics and Electrical Engineering[2] — Mechanical Engineering and Process Technology[2] — Building Technology — Fire Research — Consumer Product Technology — Field Methods.

THE INSTITUTE FOR COMPUTER SCIENCES AND TECHNOLOGY conducts research and provides scientific and technical services to aid Federal agencies in the selection, acquisition, application, and use of computer technology to improve effectiveness and economy in Government operations in accordance with Public Law 89-306 (40 U.S.C. 759), relevant Executive Orders, and other directives; carries out this mission by managing the Federal Information Processing Standards Program, developing Federal ADP standards guidelines, and managing Federal participation in ADP voluntary standardization activities; provides scientific and technological advisory services and assistance to Federal agencies; and provides the technical foundation for computer-related policies of the Federal Government. The Institute consists of the following centers:

Programming Science and Technology — Computer Systems Engineering.

[1]Headquarters and Laboratories at Gaithersburg, MD, unless otherwise noted; mailing address Washington, DC 20234.
[2]Some divisions within the center are located at Boulder, CO 80303.

Measurement of Optical Fiber Bandwidth in the Time Domain

Douglas L. Franzen
G.W. Day

Electromagnetic Technology Division
National Engineering Laboratory
National Bureau of Standards
Boulder, Colorado 80303

U.S. DEPARTMENT OF COMMERCE, Philip M. Klutznick, Secretary
Luther H. Hodges, Jr., Deputy Secretary
Jordan J. Baruch, Assistant Secretary for Science and Technology

NATIONAL BUREAU OF STANDARDS, Ernest Ambler, Director

Issued February 1980

NATIONAL BUREAU OF STANDARDS TECHNICAL NOTE 1019

Nat. Bur. Stand. (U.S.), Tech. Note 1019, 72 pages (Feb. 1980)
CODEN: NBTNAE

U.S. GOVERNMENT PRINTING OFFICE
WASHINGTON: 1980

For sale by the Superintendent of Documents, U.S. Government Printing Office, Washington, D.C. 20402
Stock No. 003-003-02161-0 Price $3.75 (Add 25 percent additional for other than U.S. mailing)

CONTENTS

MEASUREMENT OF OPTICAL FIBER BANDWIDTH IN THE TIME DOMAIN

Douglas L. Franzen
and
G.W. Day

A system is described for determining optical fiber bandwidth from time domain information. A measurement gives the optical fiber transfer function (or frequency response) relating the output waveform to the input. An analysis is given of the variables affecting the measurement. This includes a discussion of such input related topics as launching conditions, mode scramblers, and laser diode sources; output related topics include a discussion of optical detectors. Laser diodes are evaluated with respect to short pulse performance, near field emission, material dispersion limits, and other spectral behavior like chirping; detectors are evaluated with respect to time response, linearity, and uniformity. Overall system architecture, precision, and dynamic range are discussed. A number of bandwidth related topics are briefly presented and typical experimental results given. This includes examples of: mode mixing via microbending, profile compensation, profile dispersion, intramodal broadening, material dispersion constants, relative magnitude-phase behavior, and Gaussian predictions of frequency response.

Key words: Bandwidth; laser diodes; material dispersion; mode scramblers; optical detectors; optical fibers; transfer function.

1. INTRODUCTION

Attenuation and bandwidth are the important parameters used to describe the propagation characteristics of optical fiber waveguides. Measurement practices with regard to these parameters continue to evolve as accumulated practical experience and the efforts of standards groups lead toward uniformly accepted procedures. This Technical Note is one of a series intended to describe the present design and capabilities of fiber measurement systems used at the National Bureau of Standards. These systems are perhaps representative of current practice in the industry and many of the present techniques and methods will be relevant to future systems. In this Technical Note, the emphasis is on the bandwidth measurement of multimode, silica, telecommunications-type fibers over the 0.8 to 0.9 μm wavelength region. Much of the discussion is general and can be applied to most optical fiber bandwidth measurement systems.

2. BANDWIDTH CONSIDERATIONS IN OPTICAL FIBERS

2.1 Pulse Broadening in Optical Fibers

Bandwidth is related to the information carrying capacity of a fiber and includes the various sources of signal distortion. In multimode optical fibers, differences in mode group velocity result in pulse broadening or spreading; i.e., different modes arrive at the output at different times. This is commonly called "intermodal" broadening, and in multimode fibers is often the most significant bandwidth limitation [1]. Due to coupling between modes, the intermodal broadening of multimode fibers does not necessarily scale linearily with fiber length. In fact, a square root dependence is observed in cases of strong mode coupling [2].

Other sources of pulse broadening affect all of the fiber modes together. This contribution to pulse broadening is commonly called "intramodal" broadening [1]. While different modes are affected different amounts, it is often useful to think of an average intramodal term to describe a given fiber. Intramodal broadening is directly proportional to source linewidth and arises because different spectral components of the source travel with different velocities. Intramodal broadening results from both material and waveguide dispersion. Material dispersion is related to the optical properties of the fiber core material, in particular, to the second derivative of the refractive index with respect to wavelength. Waveguide dispersion is related to the physical dimensions of the core, to the index profile, and to wavelength. Because of the dependence of intramodal broadening on source linewidth, some authors have chosen the terms "monochromatic" and "chromatic" to distinguish intermodal and intramodal effects. Presently there is no standard terminology to describe the various contributions to pulse broadening. Perhaps this is because in a strict mathematical sense, the terms cannot be clearly separated.

The concept of rms pulse broadening is useful in describing the time domain behavior of pulse propagation in optical fibers [1]. The rms duration σ, of a waveform $p(t)$ is given by

$$\sigma = \left[\int_{-\infty}^{+\infty} p(t)(t-T_o)^2 \, dt \right]^{1/2} \tag{1}$$

where $p(t)$ is normalized according to

$$\int_{-\infty}^{+\infty} p(t)dt = 1 \quad , \tag{2}$$

and T_o is the central time given by

$$T_o = \int_{-\infty}^{+\infty} tp(t)dt \quad . \tag{3}$$

The rms pulse duration of the fiber impulse response, σ_T, for a fiber with input and output waveforms $p_1(t)$ and $p_2(t)$ respectively is approximated by

$$\sigma_T = \sqrt{\sigma_2^2 - \sigma_1^2} \tag{4}$$

where σ_1 and σ_2 are the corresponding rms values for the input and output waveforms. In practice, rms pulse broadening is difficult to implement because low level values near the baseline receive a large weighting in equation (1). The total rms broadening, σ_T, for a fiber can also be expressed in terms of the inter and intramodal contributions by

$$\sigma_T^2 = \sigma^2_{\text{intermodal}} + \sigma^2_{\text{intramodal}} \tag{5}$$

where $\sigma_{intermodal}$ and $\sigma_{intramodal}$ represent the rms broadenings due to the individual components.

When intramodal broadening is dominated by material dispersion, the term is given by

$$\sigma_{intramodal} = \frac{\lambda}{c} \frac{d^2n}{d\lambda^2} \sigma_s L \qquad (6)$$

where n is the on-axis refractive index of the core, σ_s is the rms value for the spectral lineshape of the source, and L the length of the fiber. In the 0.8 to 0.9 μm wavelength range, the intramodal term is dominated by material dispersion and, for silica fibers, the waveguide dispersion does not become important until the wavelength is longer than approximately 1.1 μm.

In general the importance of the various contributions to measured fiber bandwidth depends on the type of fiber, wavelength, and source linewidth. For laser diode sources and multimode silica fibers in the 0.8 to 0.9 μm wavelength region, the intermodal term usually dominates. As the bandwidth approaches multi-GHz-km values, however, the material dispersion term becomes more important.

2.2 The Transfer Function

The rms pulse broadening concept was widely used in early fiber work. Specifications are now generally based on the transfer function. In this approach, which is analogous to conventional linear network analysis, the fiber is described by a transfer function, which is assumed to be linear in optical power; i.e., if $p_1(t)$ is the input optical power as a function of time averaged over many optical periods, $p_2(t)$ is the output similarly averaged, and $P_1(f)$ and $P_2(f)$ the corresponding Fourier transforms, then the output is related to the input by

$$P_2(f) = H(f)P_1(f) \qquad (7)$$

where H(f) is the transfer function or frequency response in baseband frequency f describing the fiber. In general, the quantities in eq (7) are complex, and the transfer function can be written in polar form as

$$H(f) = M(f)e^{i\phi(f)} \tag{8}$$

with M(f) and $\phi(f)$ being real functions of frequency f.

The validity of eq (7) has been examined by others [3], [4]. Theoretical work shows that it is valid as long as the source is sufficiently incoherent; i.e., if frequency width of $P_1(f)$ is much less than the linewidth of the source. No actual experiments have been performed to check the range of validity of eq (7) in this respect. As practical sources like laser diodes become more coherent [5], the question becomes more than academic.

If eq (7) holds, conventional linear system analysis can be used. In this work, the bandwidth is determined by measuring M(f), the magnitude of the transfer function and, $\phi(f)$ the phase response, from ratios of the fast Fourier transform of output and input waveforms. Alternatively, the bandwidth could be completely specified by giving the impulse response which is just the inverse transform of H(f). Algorithms exist to accomplish this calculation if it were desired.

It is useful to derive relationships assuming Gaussian shapes for the input pulse and fiber frequency response. We shall see later (Section 6.3) that this is an acceptable approximation for some fibers. Since the Gaussian shape is invariant under Fourier transformation, simple relationships result. If the input $p_1(t)$ and output $p_2(t)$ are given by

$$p_1(t) = e^{-4\ln 2(t/\tau_1)^2} \tag{9}$$

and

$$p_2(t) = e^{-4\ln 2(t/\tau_2)^2} \tag{10}$$

which are Gaussians having a FDHM (full duration at half maximum) of τ_1 and τ_2 respectively, then the fiber frequency response is also Gaussian with the 3 dB roll-off frequency given by

$$f_{3dB} = \frac{.44}{\sqrt{\tau_2^2 - \tau_2^2}} \tag{11}$$

$$= \frac{.44}{\tau_T} \quad . \qquad (12)$$

where τ_T is the half width broadening of the fiber. Also, the rms pulse duration for a Gaussian is a simple expression with

$$\sigma_1 = .43 \quad \tau_1 \qquad (13)$$

and

$$\sigma_2 = .43 \quad \tau_2 \quad . \qquad (14)$$

Using eq (13) with eq (11), an expression can be found relating the 3 dB frequency of the transfer function, f_{3dB}, to the rms pulse broadening, σ_T, for the fiber with

$$f_{3dB} \; \sigma_T = .19 \quad . \qquad (15)$$

2.3 Important Parameters Affecting Bandwidth Measurements

Precision of fiber bandwidth measurements can be quite good for repeated measurements with the same system (e.g. section 5.1). However, certain parameters can vary among systems to cause rather large measurement discrepancies or offsets. These parameters include launching conditions, receiving conditions, and source spectral properties. Other factors, representing the limitation of commercial equipment, such as sampling oscilloscope time base non-linearity, sampling head aberration, etc. are important, but not as significant as the former problems.

Launching conditions are particularly important, because in multimode fibers, the modes exhibit differential delay and attenuation. Thus the output pulse shape depends on the specific modes excited at the input (see section 3.3). Nearly as significant as the launching conditions are the receiving conditions which determine how the modes are differentially detected (see section 3.2.4).

Source spectral properties influence the measured bandwidth via intramodal broadening (material dispersion). For normally encountered laser diode linewidths, at wavelengths of 800-900 nm, this does not become important until the fiber bandwidth exceeds 1 GHz-km (see sections 3.1.4 and 5.3). Measurements on high bandwidth fibers will therefore reflect the varability commonly encountered in laser diode linewidths.

3. DESCRIPTION OF MEASUREMENT SYSTEM

3.1 Laser Diode Sources

3.1.1 Short-Pulse Performance

Laser diodes are the most commonly used sources for optical fiber bandwidth measurements. They are relatively inexpensive, compact, and usually sufficiently incoherent to satisfy the transfer function validity requirement. Moreover, pulses that are much shorter than the electrical driving current pulses can be generated at repetition rates useful for sampling oscilloscopes. This "Q-switching" behavior is still poorly understood but is believed to be related to a saturable absorption in the optical cavity of the laser diode.

Gloge and other early workers generated short pulses from GaAs single heterojunction laser diodes by using mercury wetted reed relays to switch charged transmission lines [6, 7]. In this manner, pulses of 100 ps FDHM were produced at repetition rates of a few hundred Hz. Transistors operating in the avalanche mode can also be used as fast switches [8,9,10]. Andrews describes a useful avalanche transistor circuit for switching a charged transmission line to produce 110 ps FDHM pulses from a GaAs laser diode [9]. Dannwolf, et al., report a similar circuit with a ceramic chip capacitor as the energy storage element that produced pulses of 190 ps FDHM [10].

Compared to mercury wetted relays, avalanche transistors have the advantage of high repetition rate and external trigger capability. In the present study avalanche transistor switching circuits using both silver mica capacitors and transmission lines as the energy storage element were examined. Transmission lines were found to be preferable producing slightly narrower pulses with less tendency toward multiple pulsing.

The circuit, using five miniature coaxial cables (RG-174U), is shown in figure 3-1. When a single cable is switched across a low impedance, the current delivered is approximately $\Delta V/R$ where R is the cable characteristic impedance and ΔV the voltage swing available from the avalanche transistor.

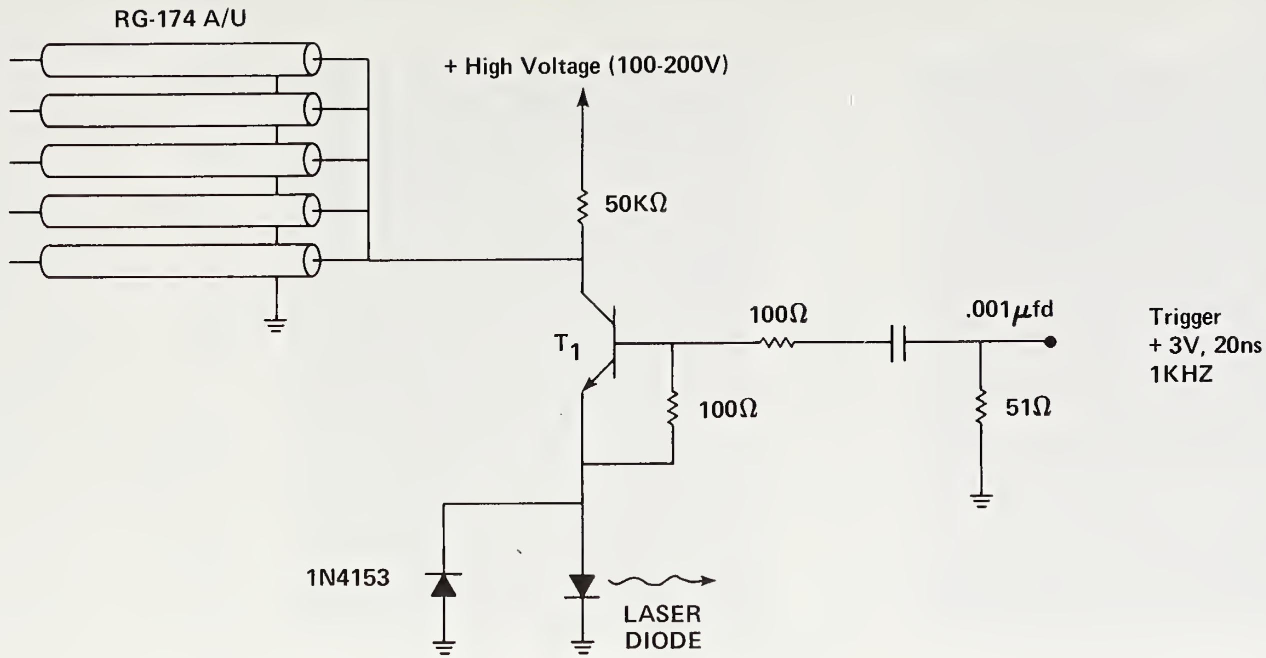

Figure 3-1. Circuit for pulsing GaAlAs and GaAs single heterojunction laser diodes.

With an R of 50 ohms, a ΔV of 150 volts, the current delivered is 3 amps. Thus, five cables are necessary to supply up to 15 amps to a diode. Two different avalanche transistors were used, a 2N3700 for high ΔV and a 2N3904 for lower ΔV. The only other circuit element requiring explanation is the diode shunting the laser diode which is intended to protect it from excessive reverse bias. The whole circuit, except for cables, is packaged in a 3x3x6 cm instrument box.

The repetition rate was arbitrarily limited to 1 kHz. While these circuits may be operated at several tens of kHz, the lower repetition rate was chosen to guard against diode aging. Several diodes have been in routine operation for over one year and no circuit failures or changes in pulse shape, threshold, jitter, wavelength, etc., have been observed.

The main factor affecting short-pulse performance is the choice of a specific laser diode; significant differences are observed among diodes of the same type and manufacturer. The objective in short pulsing is to drive the diodes sufficiently far above threshold without generating multiple pulses. Shortest pulses and least tendency toward multiple pulsing was achieved by operating near the maximum voltage for a particular transistor and with cable lengths short enough to obtain a single pulse.

Four diodes selected from a large number of RCA C30012 (GaAlAs), Laser Diode LA-63 (GaAlAs), and RCA SG2001 (GaAs) single heterojunction diodes [11] were chosen to cover the 0.8 to 0.9 µm wavelength region. These diodes had wavelengths of 803, 824, 866, and 902 nm.

A typical pulse shape is shown in figure 3-2 and consists of a nearly Gaussian-shaped main pulse of nominally 250 ps FDHM followed by a tail at 5-10% of the peak level. Table I gives the tabulated performance for all of the diodes. The frequency spectrum of the pulse is of prime importance; figure 3-3 shows a typical Fourier transform of one of the diode pulses. In obtaining this data, a delay line was used with the sampling oscilloscope; consequently, the detected pulses were broadened to about 330 ps FDHM. The 3 dB frequency is approximately 1 GHz. Observed pulse shapes do contain some broadening from the detector (section 3.2) and in some cases are probably less than 200 ps in actual duration.

It should be mentioned that the above temporal behavior and the spectral emission reported in section 3.1.4 were determined from the power exiting a short length of fiber and are therefore representative of actual system use.

3.1.2 Near-Field Radiation Patterns

The emission region in laser diodes consists of a narrow strip at the PN junction interface. In the case of C30012 and LA-63 GaAlAs diodes the

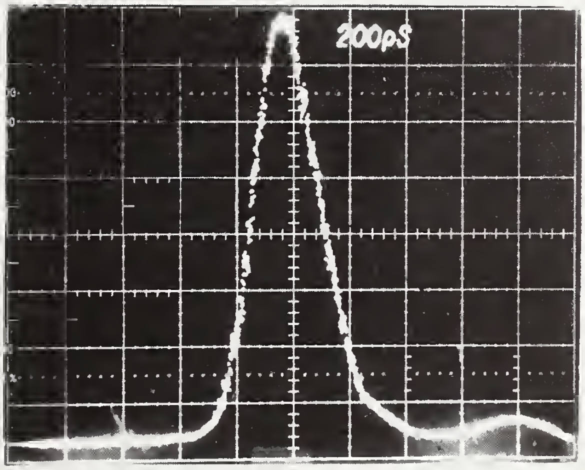

(a)

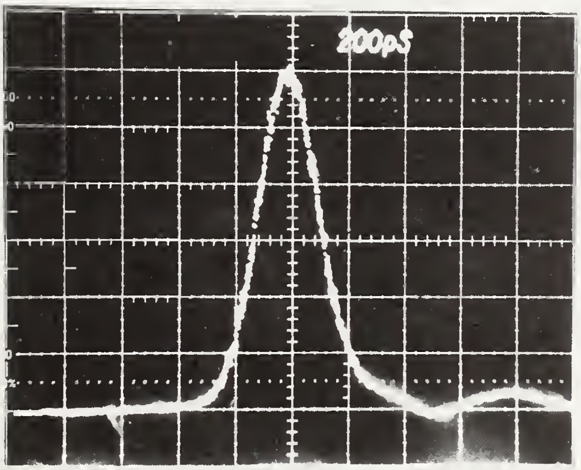

(b)

Figure 3-2. Typical pulses from single heterojunction laser diodes, 200 ps per division, (a) 824 nm GaAlAs diode, (b) 902 nm GaAs diode.

TABLE I

Laser Diode Pulse Durations

Diode	Pulse Duration, ps (FDHM)
803 nm, GaAlAs	250
824 nm, GaAlAs	240
866 nm, GaAlAs	290
902 nm, GaAs	250

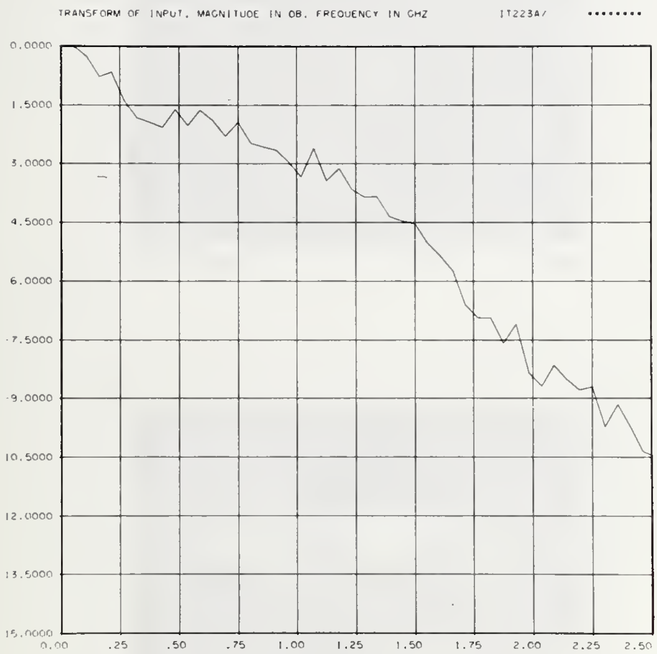

Figure 3-3. Frequency content for a typical laser diode pulse, 902 nm GaAs, 3 dB frequency approximately 1 GHz.

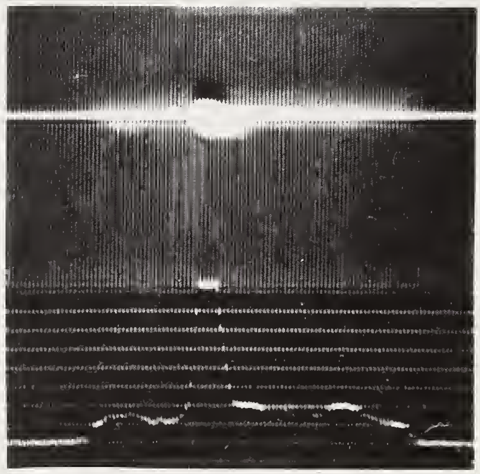

(a)

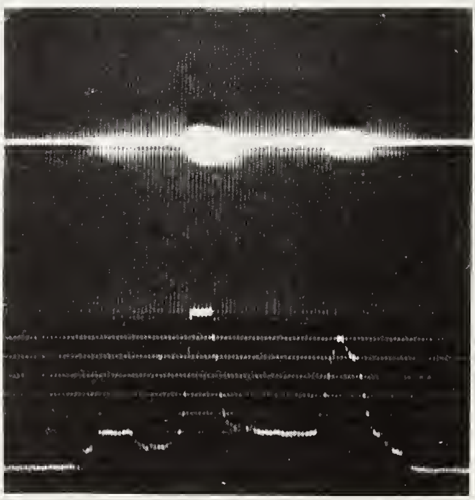

(b)

Figure 3-4. Near-field emission characteristics: (a) 803 nm GaAlAs diode operating in short-pulse mode; quantitative curve relates to intensity along scan bar (oriented along junction image). Note low level spontaneous emission along entire junction length with laser emission over a small segment; (b) Same as (a) but with inreased drive current causing other junction segments to exceed threshold.

junction dimension is 150 x 2 μm while for SG2001 GaAs diodes it is slightly smaller (75 x 2 μm). We find that the emission characteristics vary among diodes and cannot be accurately predicted. In the short-pulse mode the emission generally occurs over only a small segment of the junction. This is because the diodes are operated close to threshold and only the lowest loss regions of the junction oscillate. Typical behavior is given in figure 3-4 for the 803 nm diode. Figure 3-4(a) is an image of the junction showing low level spontaneous emission along the entire 150 μm junction length. Laser emission is restricted to a 16 μm segment of the total length. However, if the diode is driven further above threshold, other parts of the junction will eventually oscillate, as shown in figure 3-4(b). All of the diodes exhibit this behavior except for the 824 nm diode which oscillates over a 40 μm length of the junction immediately from threshold.

3.1.3 Launched Power

The amount of power launched into a fiber is important since it affects signal to noise ratio. Power launched into a fiber with the diodes operating in the short-pulse mode was determined using two different types of calibrated detectors. One detector responded to individual pulse energy (in the 10 picojoule range) while the other measured total average power (10 nanowatt range). Measurements on the 825 nm diode differed by less than 10%. Peak power launched into a short section of step index fiber (55 μm dia. core, .25 NA) for the different diodes is tabulated in Table II and is between 30 and 300 mW.

3.1.4 Spectral Emission

Spectral emission properties of the source are important because they determine the extent of intramodal pulse broadening in the fiber. The output of laser diode source consists of both spontaneous emission (linewidth about 30 nm) and stimulated emission (linewidth about 1 to 2 nm). For measurement purposes, it is important that the spectrally narrow stimulated emission dominate. Figure 3-5(a) shows the pulse shape which is coupled into a short length of fiber with the diode operated just below threshold. The pulse width is about 5 ns and the cusp represents the short pulse starting to form from stimulated emission. Above threshold, figure 3-5(b) the short pulse is fully produced with the peak power exceeding the spontaneous emission by a factor of 70 for this particular diode. Contributions from spontaneous emission were judged to be insignificant for all diodes tested.

Spectral lineshapes were determined using time resolved measurements. This was necessary to determine the extent of "chirping," a shift of

TABLE II

Peak Power From Laser Diodes Exiting a Short Length of Step Index Fiber with Mode-Scrambler

Diode	Peak Power, mW
803 nm, GaAlAs	150
824 nm, GaAlAs	300
866 nm, GaAlAs	65
902 nm, GaAs	35

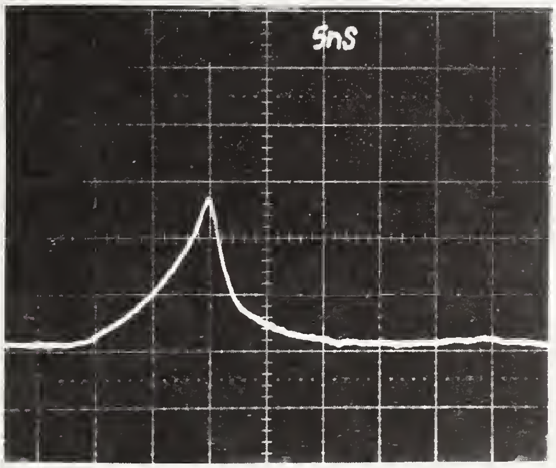

(a)

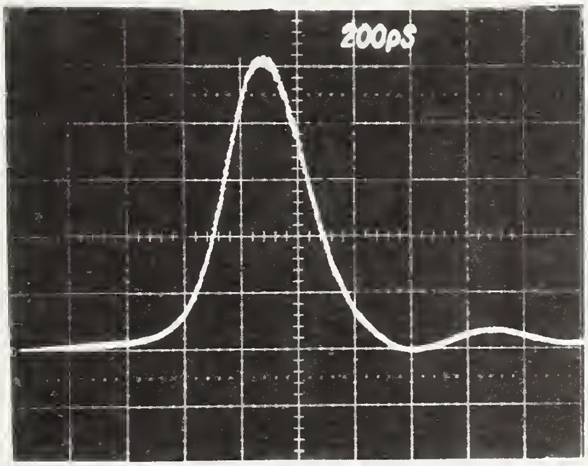

(b)

Figure 3-5. (a) Spontaneous emission coupled into fiber (laser diode below threshold), 5 ns per division. (b) Laser emission coupled into fiber (laser diode above threshold); 200 ps per division; peak power in (b) is 70 times that in (a).

instantaneous spectral emission with time that can affect bandwidth measurements [12]. Radiation from the diodes was coupled into a short length of fiber containing a mode scrambler (section 3.3); after relaunching into a second fiber, the radiation was passed through a monochrometer and onto a detector (BPW-28, section 3.2). By triggering the sampling oscilloscope externally with a signal derived from the electrical trigger to the laser diode, a dc signal was obtained that was proportional to optical power at a selected point in time. Optical power was recorded on a strip chart recorder while the monochrometer was scanned. Line shapes were recorded on the leading half-height of the pulse and on the trailing half height. Only the 824 nm diode showed a significant shift of line center during the pulse, figure 3-6. During the pulse, the peak of the spectral emission moved 0.7 nm toward longer wavelength. This rate of chirping, 0.0027 nm/ps, is not very different from the 0.0018 nm/ps previously reported for sub-nanosecond pulses from a particular single heterojunction laser diode [12]. The 824 nm diode differed from the rest in that it was driven higher above threshold with more of the junction stripe oscillating. This observation seems to be consistent with the evidence in [12] that chirping results from filaments in the junction stripe having different wavelengths and time delays.

The spectral shapes from the four diodes showed different behavior; some were smooth Gaussian-like while others consisted of several partially resolved cavity modes. An example of the latter behavior was the 902 nm diode, figure 3-7, where several modes of the diode were partially resolved by the monochrometer. Figure 3-7 was obtained using a detector having a 5 ns FDHM impulse response and therefore represents pulse energy.

Lineshapes for a given diode with a fixed alignment showed good reproducibility. However, fine structure changes within a nominal shape could be observed with different alignments of the diode. Nominal behavior for the four diodes is summarized in Table III.

3.2 Detectors

3.2.1 Mounting Configuration and Electrical Circuit

A number of different detectors are available for optical fiber bandwidth measurements. In the 800-900 nm region these principally include silicon PIN and APD (avalanche photo diode) devices.

A detector which performed satisfactorily was an AEG Telefunken BPW-28, silicon avalanche photodiode [11]. This detector was mounted in a structure similar to that described by Green [13], figure 3-8. In this structure the photodiode is mounted directly on the end of a coaxial transmission line

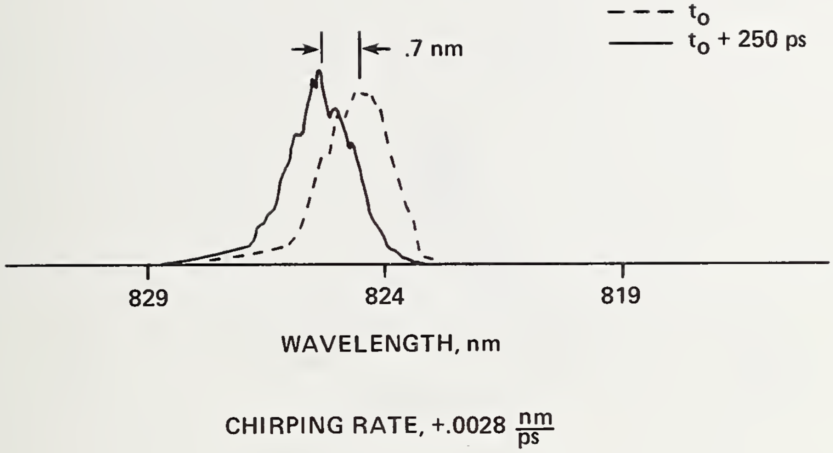

Figure 3-6. Time resolved spectral emission showing chirping behavior of 824 nm GaAlAs diode under normal short-pulse conditions. Dashed curve is a spectrum at time t_o at the front half height while solid curve is a spectrum 250 ps later at back half height (note wavelength increase to left).

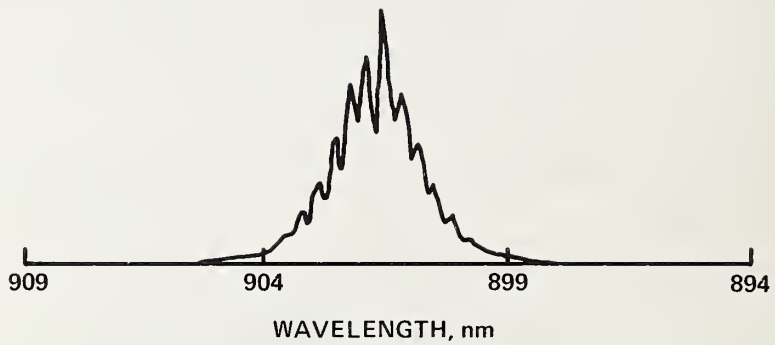

Figure 3-7. Time integrated spectral emission from 902 nm GaAs diode showing partially resolved modes.

TABLE III

Laser Diode Spectral Lineshapes

Diode	Linewidth, nm (FWHM)	General Features
803 nm, GaAlAs	1.2	Smooth with some mode structure
824 nm, GaAlAs*	1.6	Smooth, Gaussian like
866 nm, GaAlAs	.9	Two completely resolved cavity modes
902 nm, GaAs	1.5	Several partially resolved cavity modes

* Only diode which exhibited measurable chirping.

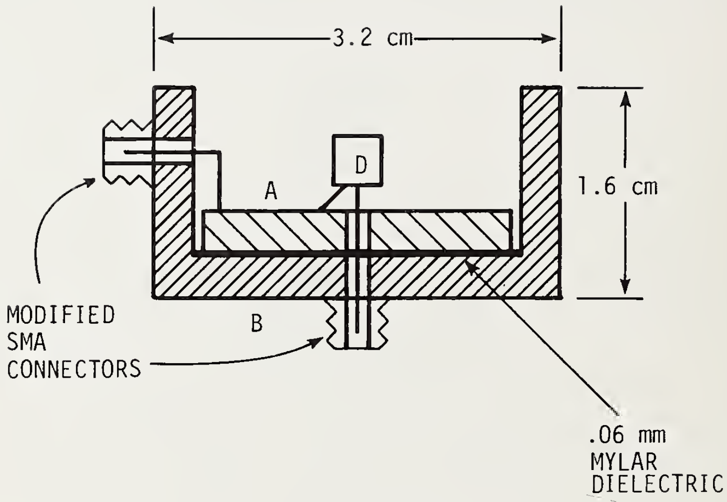

Figure 3-8. Mounting structure for optical detector, diode indicated by part D.

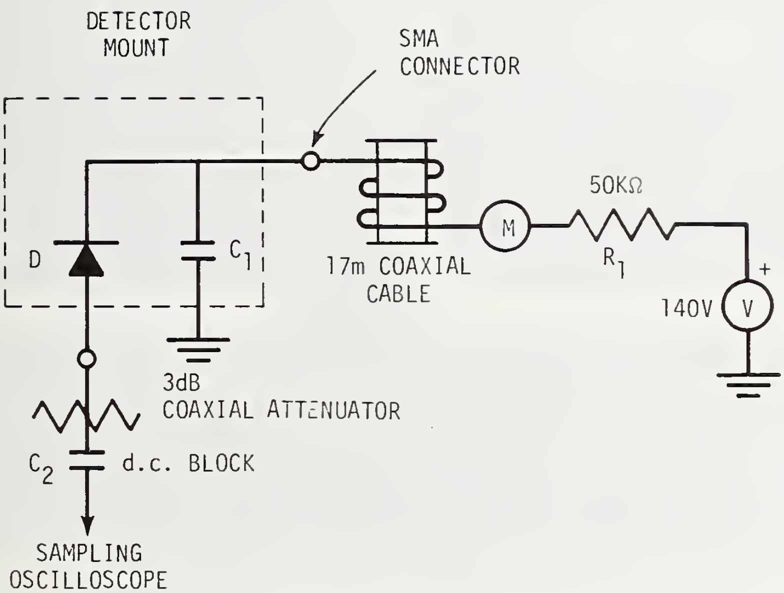

Figure 3-9. Detector electrical schematic, parts integral to mounting structure are enclosed by dashed line.

which is also coaxial with a disc capacitor. The low inductance disc capacitor, C_1, is formed by pieces A and B which are separated by a thin dielectric (.06 mm mylar). This capacitor is charged through 17 m of RG-58AU coaxial cable. Any reflections from the bias supply are therefore delayed by 160 ns and do not appear in the time window of interest. Figure 3-9 shows the complete electrical schematic. The cable is charged through resistor R_1 and ammeter M. R_1 is typically 50 kΩ and limits the current in case of an accidental short circuit. The value of R_1 and the capacitance of the cable are low enough so the cable is completely charged between pulses. Ammeter M measures the average current being supplied to the diode and is a useful monitor when approaching avalanche breakdown. Under typical operating bias, however, the average current is too low to be measured by the meter.

The detector load is a 3 dB SMA attenuator followed by an SMA series blocking capacitor. This attenuator is permanently attached to the detector and provides a constant 50 Ω load; thus, sensitive electronics can be reconnected to the detector without danger from excessive dc voltages which could occur under open circuit conditions. Blocking capacitor C_2 assures no dc voltage appears aross the sampling oscilloscope. C_2 is sufficiently large so normally encountered pulse shapes are not distorted.

3.2.2 Time Response

Ideally, detector time response should be fast compared to source pulse duration. Additional pulse broadening due to the detector will limit the upper bandwidth capability of the measuring system. Since the Fourier transform of the input pulse is the important quantity, the total pulse shape including half-duration, tail, ringing, etc., is important. It is of little use to obtain a small half-duration and yet have significant ringing. A well-matched detector is better for bandwidth measurements, and also for differential mode delay measurements where reflections could be confused with mode delay information.

A BPW-28 detector in the previously described mount was evaluated using a 1.06 μm, CW, modelocked Nd:YAG laser [14]. This laser produced pulses of 100 ps FDHM as measured with a fast detector based on a Shottky barrier-switching diode [13]. Although this detector is fast, it was not sensitive enough to use for fiber measurements with laser diode sources. Response of the BPW-28 to the modelocked pulses is shown in figure 3-10. The inferred impulse response is less than 200 ps FDHM. Notice that there is no evidence of a significant tail or ringing. These measurements were made at the 140-V bias voltage used in normal operation. The value of bias was selected by increasing the voltage until the pulse exhibited additional broadening; this

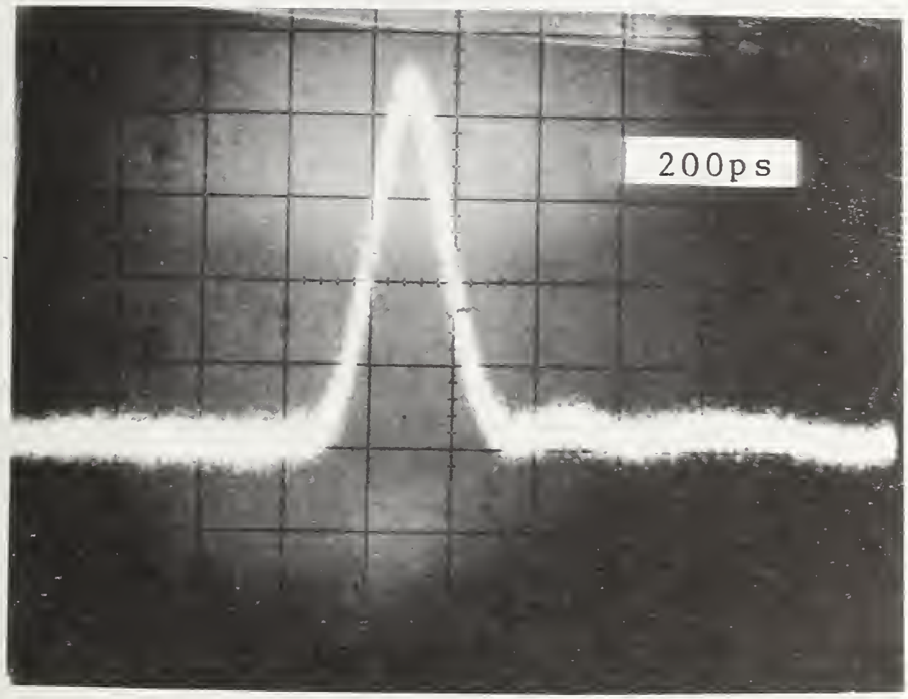

Figure 3-10. Response of BPW-28 detector to 100 ps FDHM pulse from CW modelocked, 1.06 μm, Nd:YAG laser, 200 ps per division.

yielded an avalanche gain of less than 10. This is substantially below the maximum available gain and is consistent with the gain-bandwidth trade-off in APD detectors.

3.2.3 Linearity

To obtain the frequency response of optical fibers, the output pulse must be compared to the input pulse. This requires that all components be linear, and in particular that the optical power levels involved not saturate the detector. Since the power of the input pulse is substantially higher than that of the output, a variable optical attenuator is used in front of the detector to control peak power. Thus, the detector is not used over a very large range of powers. It is also positioned in the exit optics so its aperture is filled; therefore, the power density (irradiance) on the detector is minimized.

The detector was tested for linearity at the highest levels used in the measurement system (8 ma peak diode current). This was done by varying the optical power by a factor of more than three and comparing the detected pulse shapes at the different powers. The whole pulse shape is checked for saturation. Figure 3-11 shows the normalized comparison; each pulse was digitally acquired from the sampling oscilloscope with each point being the analogue average of several hundred pulses. As indicated, there is no appreciable difference between the pulses at the two power levels. Linearity of this particular detector was thus judged to be adequate.

3.2.4 Uniformity

The detector response should be uniform across the sensitive area. If this is not the case, then preferential mode detection can take place. Concern is usually expressed over launching conditions to a fiber; however, in the absence of much mode coupling, the receiving conditions are just as important. In fact, the spatial information at the output using an overfilled input is often used to make differential mode delay measurements [15]. Recent studies have shown that the responses of several commercial APD detectors are not necessarily uniform [16]. Consequently, the detector uniformity was investigated.

The BPW-28 detector has a circular sensitive area .2 mm in diameter surrounded by a ring electrode, figure 3-12(a). A two-dimensional raster scan of dc responsivity was made at .63 μm, figure 3-12(b). The response was constant to ± 5% across the sensitive area. A low-level annulus was also present and corresponds to the area outside of the ring electrode.

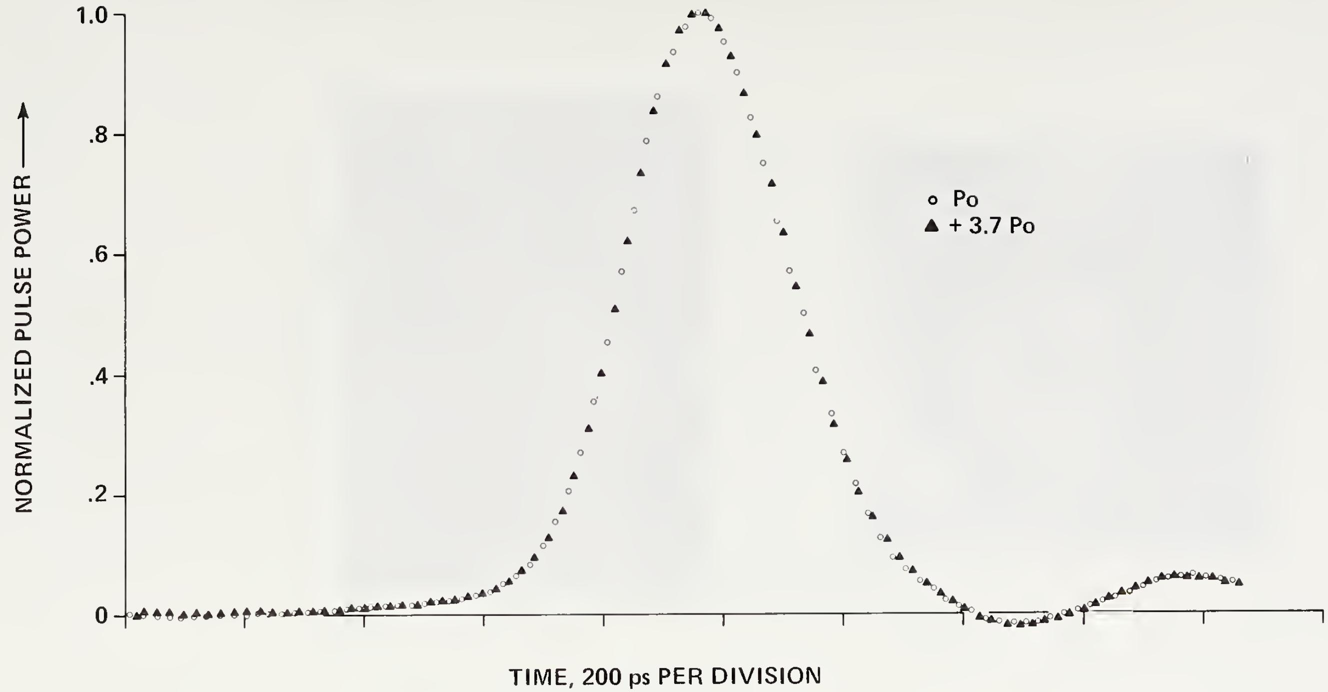

Figure 3-11. Verification of detector linearity; pulses at two different power levels show good super-position.

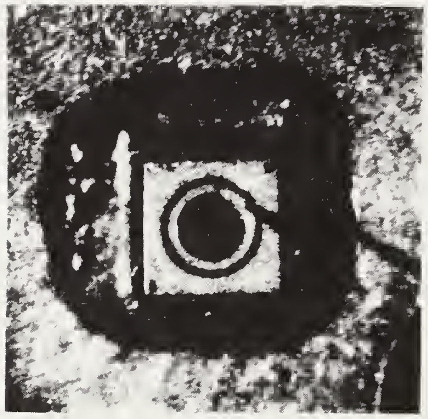

(a)

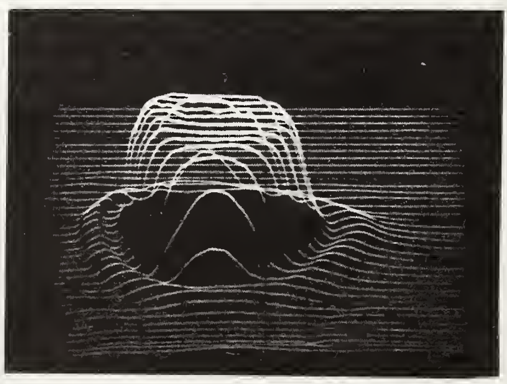

(b)

Figure 3-12 (a) BPW-28 detector, 200 μm sensitive area inside ring electrode. (b) Detector uniformity, two dimensional d.c. scan at .63 μm wavelength.

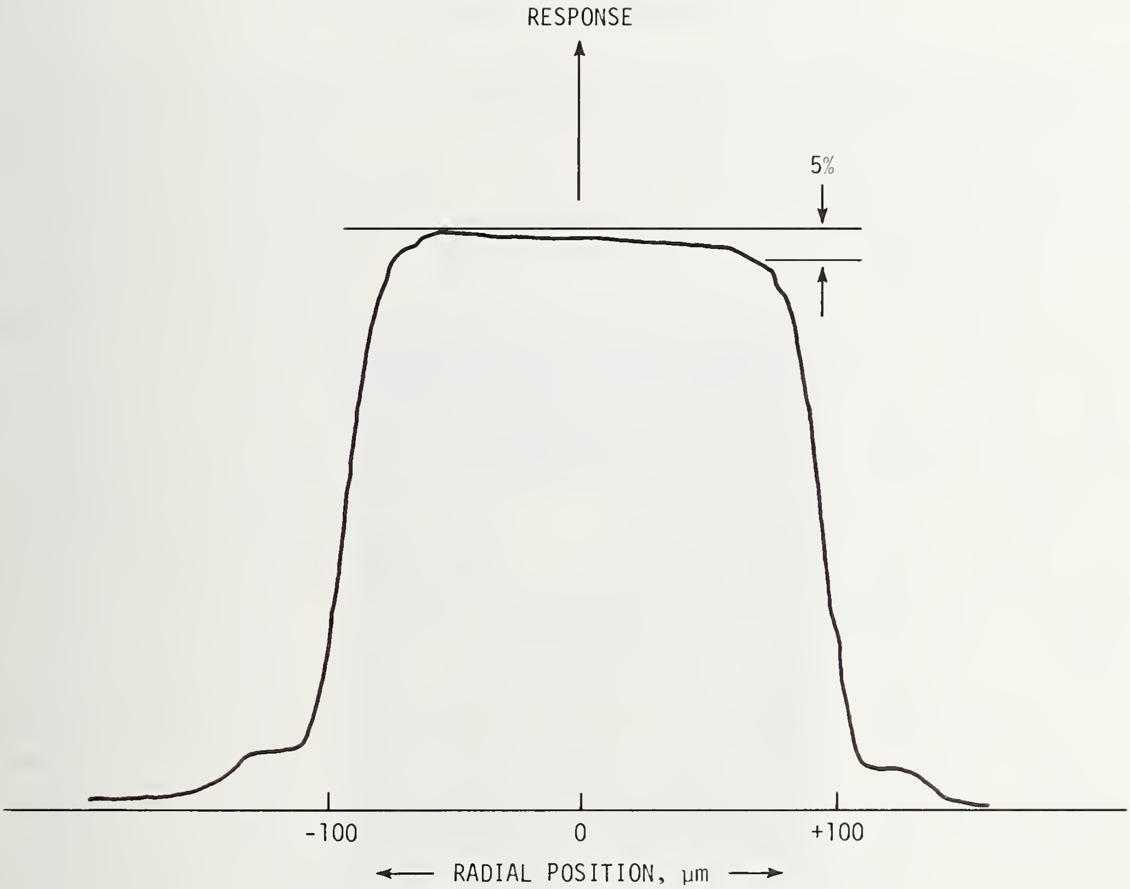

Figure 3-13. Detector uniformity, detected peak pulse power as a function of radial position.

Responsivity was also measured at high frequency. To accomplish this, a 300 ps FDHM pulse from a laser diode was focused to a 25 μm spot. This spot was scanned in one dimension across the detector and the peak power was obtained as a function of radial position, figure 3-13. As indicated, the response was flat to better than 5%. Other parts of the detector were manually scanned and similar results obtained. Detector uniformity was judged to be adequate for the present system.

3.3 Launching Conditions

Launching conditions determine the initial modes excited in a fiber. Because of differential mode attenuation and delay, the results of bandwidth measurements depend upon launching conditions. As was discussed in section 3.1.2, the emission pattern from short pulse, single heterojunction laser diodes cannot be accurately predicted and would give non-quantifiable launching conditions. To circumvent this problem, a mode scrambler is used in a 2m section of step index fiber and the radiation relaunched to provide a well-defined launching condition [17].

The mode scrambler, which is conceptually similar to previous serpentine designs [18], consists of 7 nylon posts 1 cm in diameter, placed on 1.3 cm centers, figure 3-14(a). Three of the posts are positioned on a translation stage and can be moved into alignment with the rest. In this manner a fiber can be placed in the mode scrambler without breaking since the bending radius is never less than that of the posts.

Without the mode scrambler, various near-field patterns could be obtained from the step fiber depending upon diode alignment. Patterns ranged from on-axis maximums to annular shapes. With the mode scrambler, the near-field patterns were more uniform and not as sensitive to diode alignment. With proper alignment, the near-field emission could be made very uniform, figure 3-14(b). The resulting emission from the step fiber (55 μm, .25 NA) was imaged 1:1 by two microscope objectives and relaunched into the fiber under test with peak transmitted power being the alignment criterion. For this alignment,the image of the step fiber is not necessarily exactly at the input end of the test fiber; however, for overfilled launching conditions, this does not represent a significant uncertainty. This launching overfills the modes of most fibers and results in a bandwidth which is lower than that obtained with small spot excitation. The advantages of the overfilled launching condition are: 1) it can be reproduced in other laboratories and 2) it is the starting point for other types of launching conditions which make use of equilibrium mode simulators on the fiber under test.

A comparison was made using two different launching conditions on the

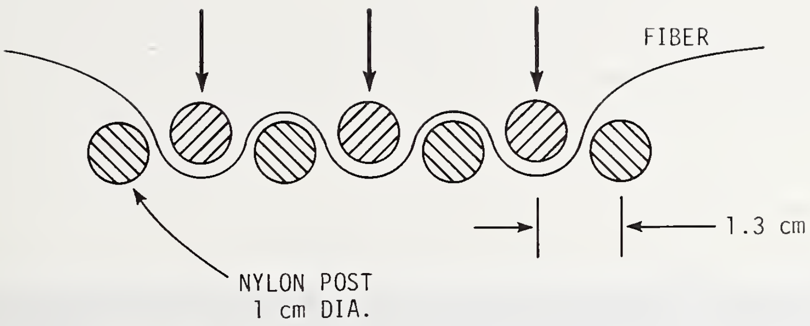

(a)

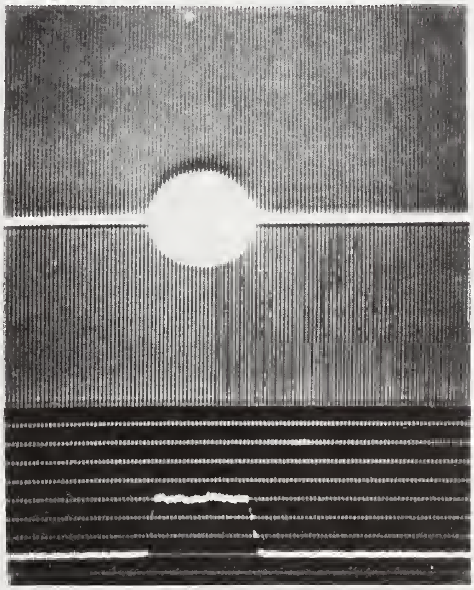

(b)

Figure 3-14. (a) Serpentine mode scrambler used in a 2 m section of step index fiber (55 μm core, .25 NA). (b) Near-field emission from step fiber with mode scrambler adjusted to give most uniform pattern--curve relates to intensity along scan bar.

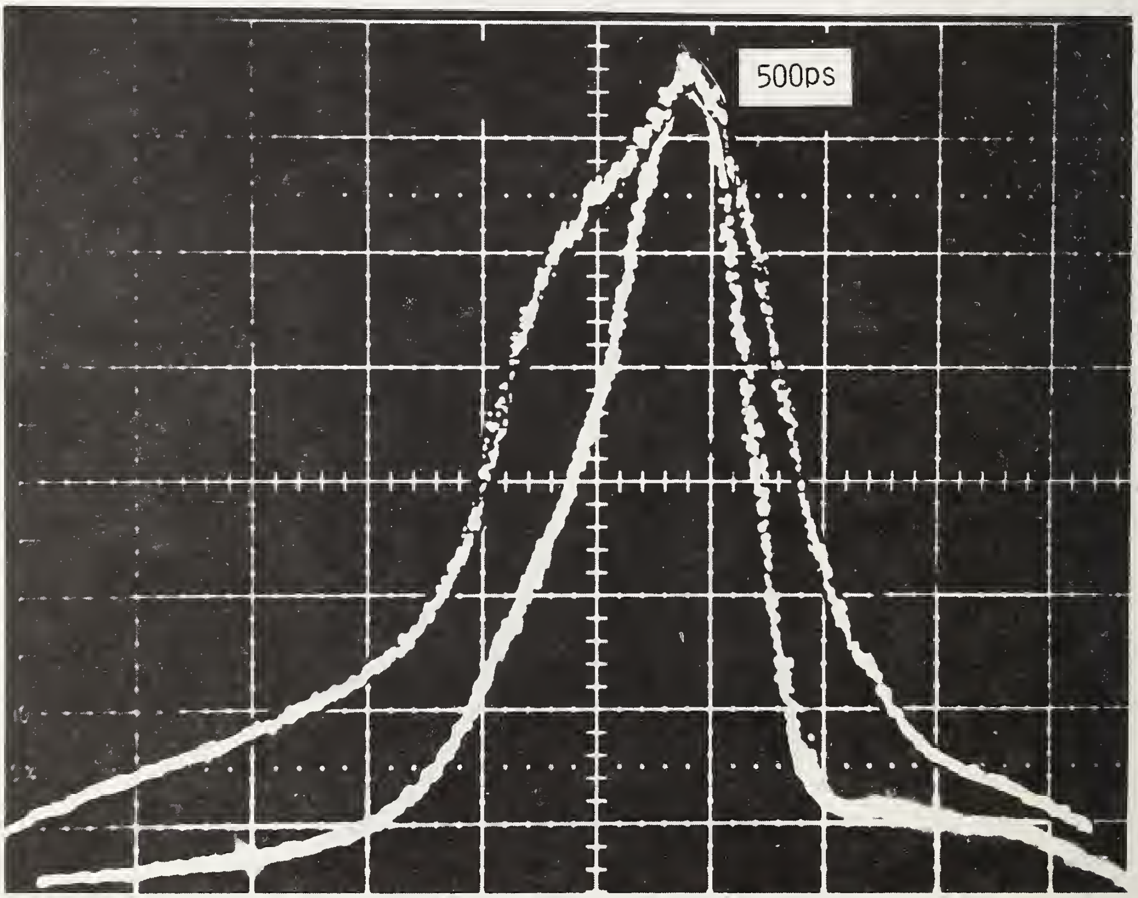

Figure 3-15. Superimposed output pulses from 1.3 km, graded index fiber using the same source (300 ps FDHM) but with different launching conditions, 500 ps per division. Narrow pulse is from directly imaging laser diode onto fiber whereas broad pulse results from use of the mode scrambler - step fiber. In both cases peak detected power was used as the alignment criteria.

same fiber with peak transmitted power being the alignment criteria. In one case the laser diode output was directly imaged onto the fiber while in the other it was first passed through the mode scrambler-step fiber filter. A superposition of the output pulses, figure 3-15, shows that the small spot from the laser diode excites fewer modes (narrower pulse) than the mode scrambler-step fiber launch which fills the mode volume of the fiber. For the two different launching conditions, the fiber half-duration broadening differs by a factor of 1.8.

An oil filled capillary is utilized to hold fibers, figure 3-16, [19]. The capillary bore is 150 μm in diameter and readily accepts standard 125 μm O.D. fibers. One end of the capillary is flared to accept the fiber while the other end has an oil reservoir covered by a thin microscope cover slip. This holder has the following advantages: 1) it acts as a cladding mode stripper, 2) the oil index matches the fiber end, and 3) it aligns the fiber stabily in the system with little readjustment required when fibers are changed. The main disadvantage is the possible accumulation of dirt and other foreign material in the capillary. For this reason the holder is demountable and the capillary can be cleaned by a thin wire.

3.4 System Architecture

The previously described components are assembled in the following manner, figure 3-17. Multiple laser diodes are mounted on a translation stage enabling different wavelengths to be easily launched into the step fiber-mode scrambler. The output from the step fiber is collimated, passed through an aperture wheel, and relaunched into the fiber under test.

A bandwidth measurement on a fiber is made by aligning the fiber for peak transmitted power and then acquiring the output waveform. Next, without disturbing the launching, the fiber is cleaved approximately 1.5 m from the input end and the waveform exiting the short length measured. This waveform is used as the input to the fiber under test.

At the receiving end, the output is collimated by a X10, .25 NA microscope objective. At this point neutral density filters are inserted to attenuate the power until it is within the linear range of the detector. Also, to minimize detector dynamic range requirements, the peak power from the short length is made equal to the power detected from the full length. Finally, the collimated output is focused on the detector by a X5 microscope objective.

Waveforms are acquired using a sampling oscilloscope. A number of choices, figure 3-18, are available for triggering the oscilloscope. First, figure 3-18(a), a digital time delay generator can be used to produce an

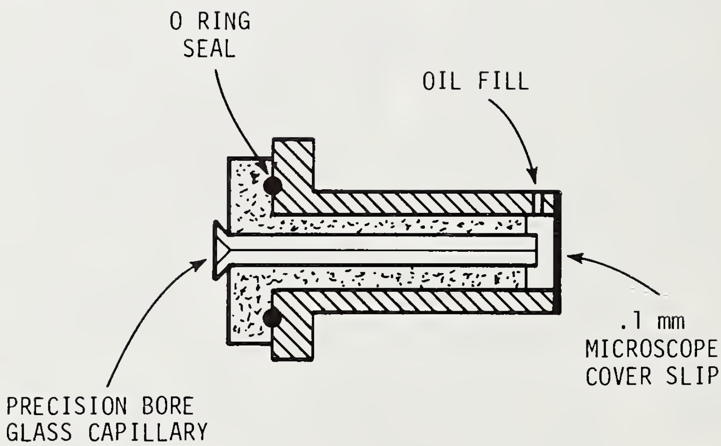

Figure 3-16. Oil filled, precision 150 μm bore, capillary fiber holder.

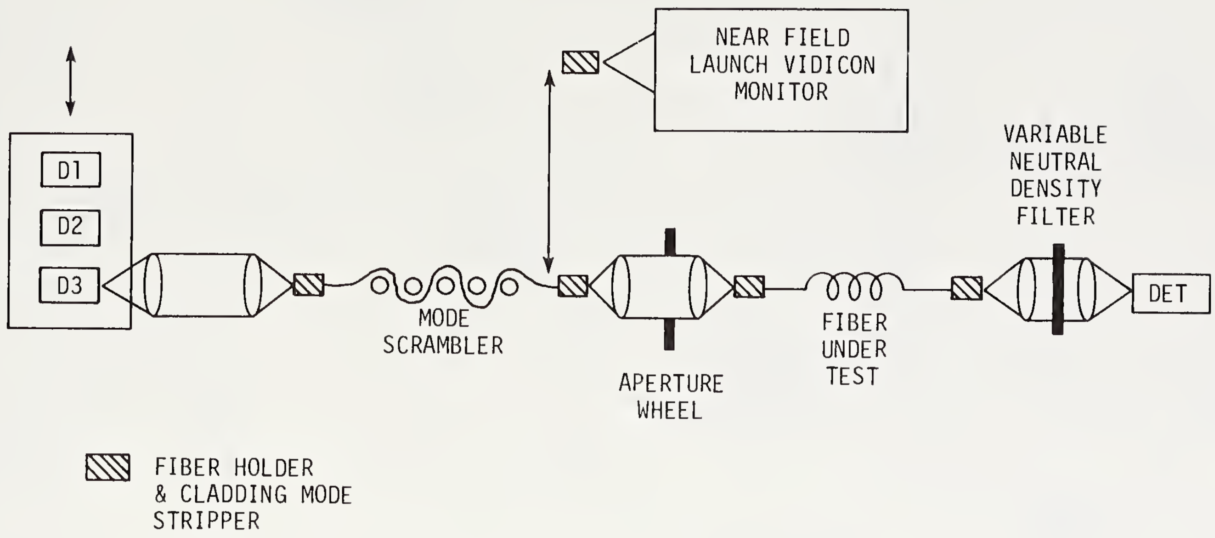

Figure 3-17. Configuration of bandwidth measurement system.

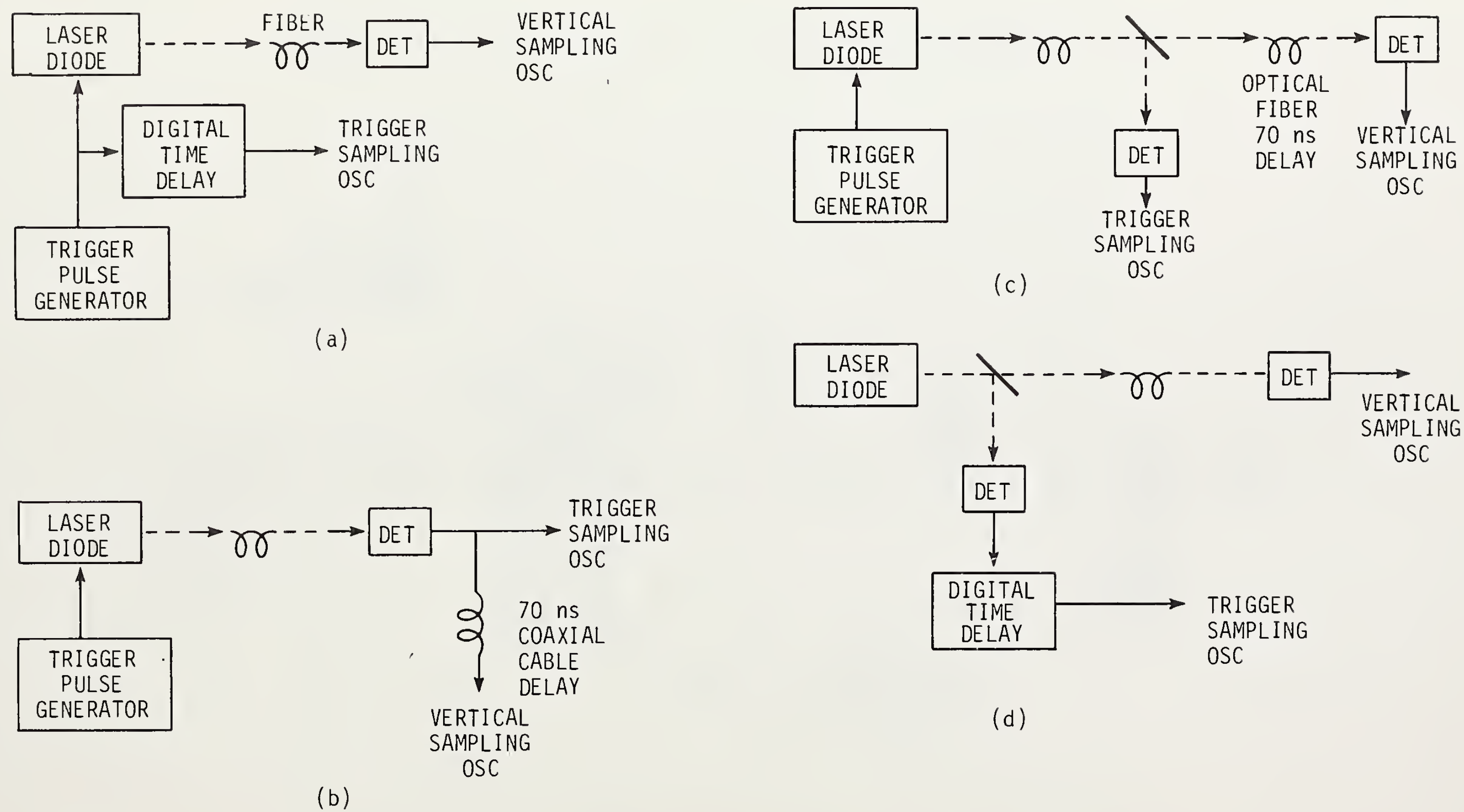

Figure 3-18. Possible choices for triggering sampling oscilloscope: (a) digital time delay generator, (b) electrical delay line, (c) optical delay line and (d) digital time delay generator scheme when source exhibits excessive trigger jitter. Dashed lines refer to optical paths hile solid lines are electrical.

electrical trigger pulse which just precedes the arrival of the optical output pulse. For this method to be successful, the delayed trigger signal must have low jitter and what jitter remains should be random so it can be averaged out. Also, the range of available delays should cover all fiber length encountered. Second, figure 3-18(b), an electrical delay line can be used at the output to delay the detected electrical signal while providing an advanced trigger signal. The delay line should have sufficient bandwidth to not appreciably distort the pulse. Third, figure 3-18(c), the optical output can be divided to provide an advanced trigger signal and then delayed optically in another fiber. This has the advantage of high bandwidth in the delay line but care must be taken to prevent the loss of modes on relaunching. Fourth, figure 3-18(d), the optical input can be divided to trigger a digital time delay generator. This configuration is useful when a digital delay is required but, the laser diode exhibits excessive trigger jitter. In the present system we utilize figure 3-18(b) with a Tektronix 7M11 delay line. To observe differential mode delay, however, figure 3-18(b) is not applicable and the method of figure 3-18(a) is used.

To digitally record a waveform, the sampling oscilloscope time base is swept by a ramp voltage while two four and one-half digit, digital voltmeters read the vertical out signal and the time base ramp. Analogue averaging is used to increase the signal to noise ratio and is accomplished with a capacitor in parallel with the vertical output to give a time constant of .2 s. Consequently, a vertical data point is the result of several hundred pulses averaged. A number of choices involving different levels of automation are available for storing data points and taking fast Fourier transforms (FFT). A description of these is beyond the intended scope of this report [20,21]. The system, in its present state, uses a large general purpose computer to compute the transforms.

4. DATA TRANSFORMATION AND ANALYSIS

4.1 General Description

Data from the acquisition system appears in the form of a 2xN integer array identified as Y(I), T(I) where Y(I) is related to the pulse amplitude and T(I) is related to time. In most cases the array is 256 elements long, a choice resulting from several compromises. Y(I) varies from about -7200 to +7200 and T(I) from +0000 to +9500 so that, in each case, the resolution in sampling the waveform is about $1{:}10^4$.

Two such arrays result from a single measurement, one representing the

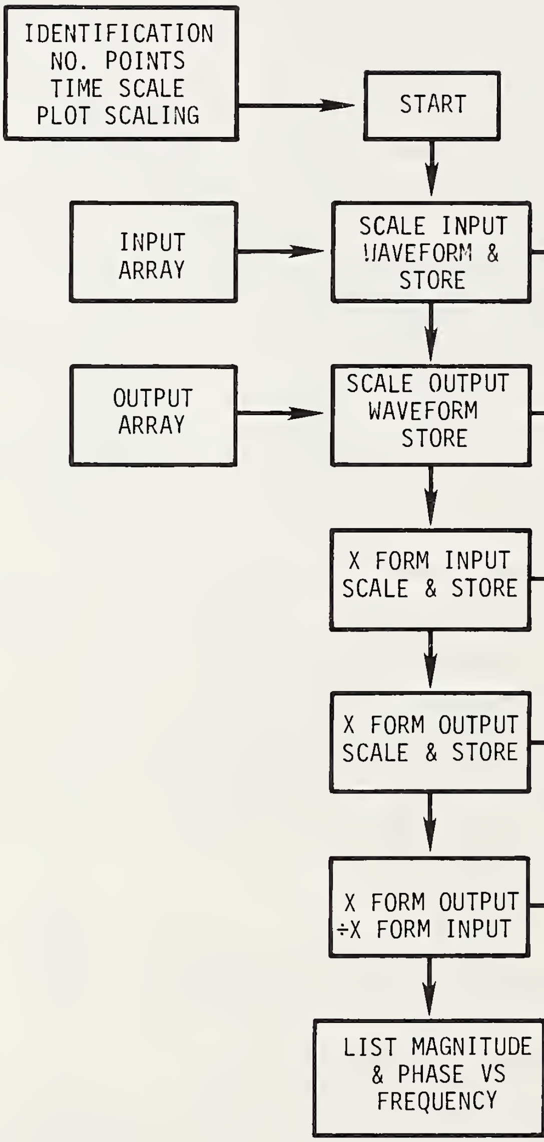

Figure 4-1. Flow diagram showing various computer program outputs.

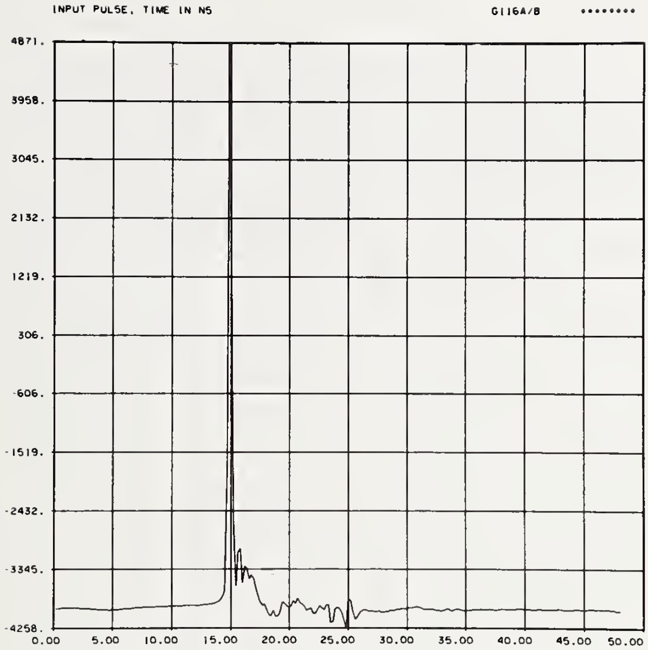

(a)

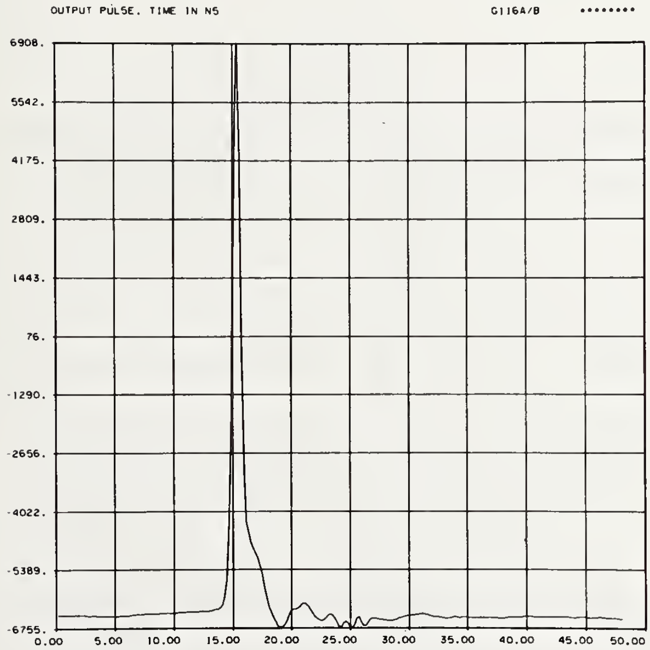

(b)

Figure 4-2. Typical set of computer generated output for a fiber bandwidth measurement: (a) input pulse (time), (b) output pulse (time), (c) Fourier transform of input pulse, (d) Fourier transform of output pulse, (e) magnitude of fiber transfer function, and (f) phase of fiber transfer function.

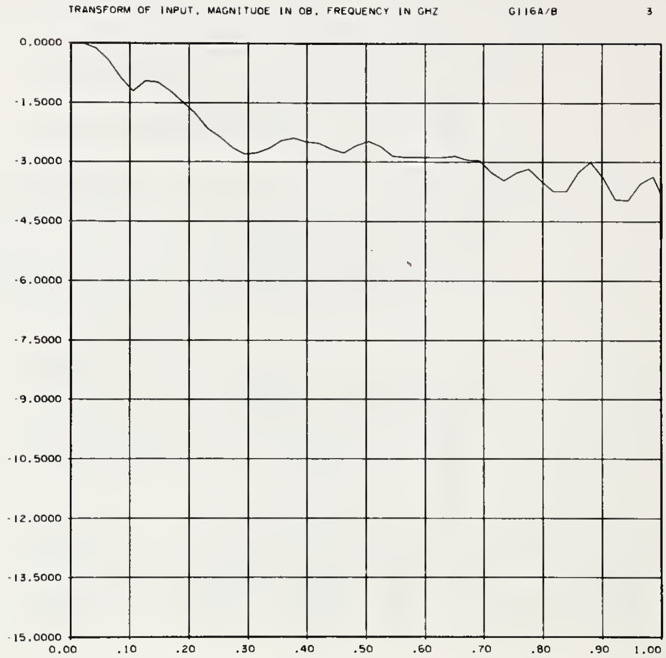

TRANSFORM OF INPUT, MAGNITUDE IN DB, FREQUENCY IN GHZ
G116A/B
3
0.0000
-1.5000
-3.0000
-4.5000
-6.0000
-7.5000
-9.0000
-10.5000
-12.0000
-13.5000
-15.0000
0.00
.10
.20
.30
.40
.50
.60
.70
.80
.90
1.00

(c)

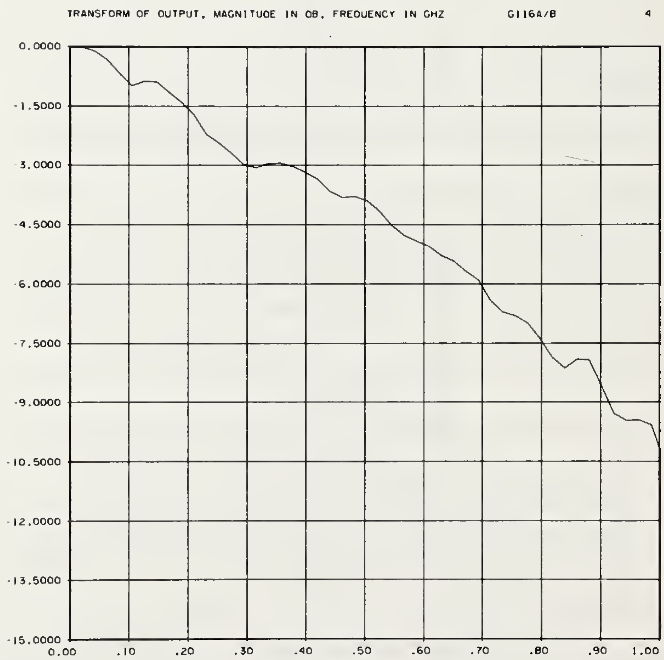

TRANSFORM OF OUTPUT, MAGNITUDE IN DB, FREQUENCY IN GHZ
G116A/B
4
0.0000
-1.5000
-3.0000
-4.5000
-6.0000
-7.5000
-9.0000
-10.5000
-12.0000
-13.5000
-15.0000
0.00
.10
.20
.30
.40
.50
.60
.70
.80
.90
1.00

(d)

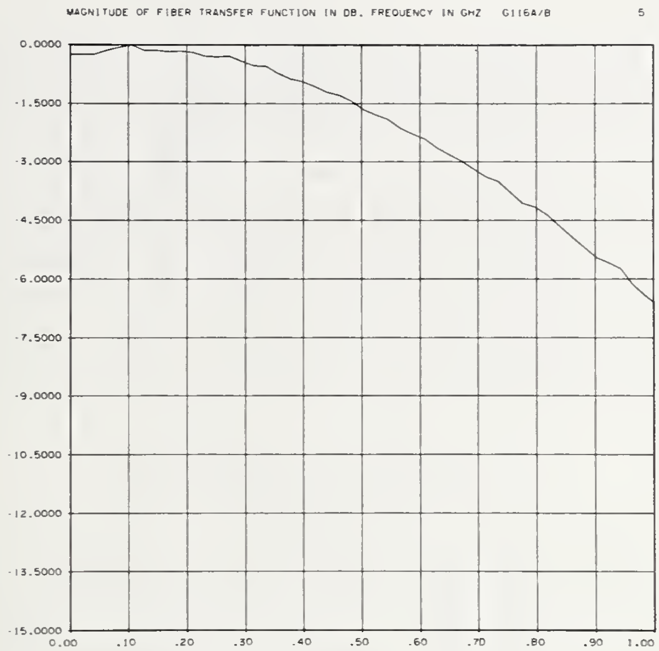
MAGNITUDE OF FIBER TRANSFER FUNCTION IN DB. FREQUENCY IN GHZ G116A/B
5
0.0000
-1.5000
-3.0000
-4.5000
-6.0000
-7.5000
-9.0000
-10.5000
-12.0000
-13.5000
-15.0000
0.00
.10
.20
.30
.40
.50
.60
.70
.80
.90
1.00

(e)

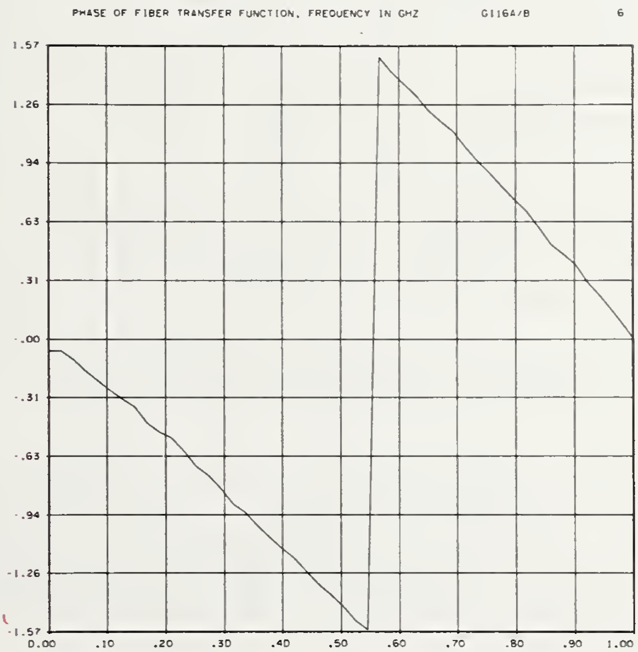
PHASE OF FIBER TRANSFER FUNCTION. FREQUENCY IN GHZ
G116A/B
6
1.57
1.26
.94
.63
.31
-.00
-.31
-.63
-.94
-1.26
-1.57
0.00
.10
.20
.30
.40
.50
.60
.70
.80
.90
1.00

(f)

input waveform and the other the output waveform. These arrays are stored in the mass storage of a large, multipurpose computer, for subsequent processing.

The analysis program provides for the scaling of both waveforms, the Fourier transformation of each, and the computation of the complex ratio of the transform of the output to the transform of the input (the transfer function). Figure 4.1 indicates the order in which these functions are carried out. Typical outputs for one fiber are shown in figure 4.2.

The Fast Fourier Transform (FFT) subroutine is a general purpose routine locally available. It is distinguished by its general versatility and by the fact that the input array need not be an integer power of two long, although that restriction greatly increases the efficiency.

4.2 Accuracy Considerations

The principal factor in assuring accurate computation of the transfer function is the choice of appropriate sampling parameters, specifically N, the number of samples, and T, the time interval between samples. The time interval must be chosen so that the transform is effectively zero at frequencies greater than $f = 1/2T$. Errors resulting from a failure to satisfy this condition are known as aliasing. Resolution in the frequency domain, that is, the frequency interval betweens points is given by $\Delta f = 1/NT$. Maintaining good resolution without introducing significant aliasing errors or requiring a particularly large number of samples thus requires certain compromises.

Because the system in its present configuration uses slow data aquisition equipment, the number of samples is generally limited to no more than 256. These samples are spaced across about 95% of the sweeptime of the sampling oscilloscope. Most fibers measured with this system have a 3 dB bandwidth below 800 MHz. In this case a 50 ns sweep is used so that $T = 0.186$ ns and $\Delta f = 21$ MHz. For higher bandwidth fibers, a 20 ns or 10 ns sweep is used.

The greatest problem with aliasing errors occurs when transforming the input waveform using the longest sweep time. Figure 4.3(a) shows the transform of a typical input pulse with the frequency range expanded to $f=1/2T$ or 2.7 GHz. At this frequency the magnitude is approximately 10 dB below its value at low frequency.

To estimate the magnitude of the aliasing error in this waveform, a sampled Gaussian pulse having a similar 10 dB bandwidth was generated and transformed. Figure 4.3(b) shows the magnitude of the transform and the

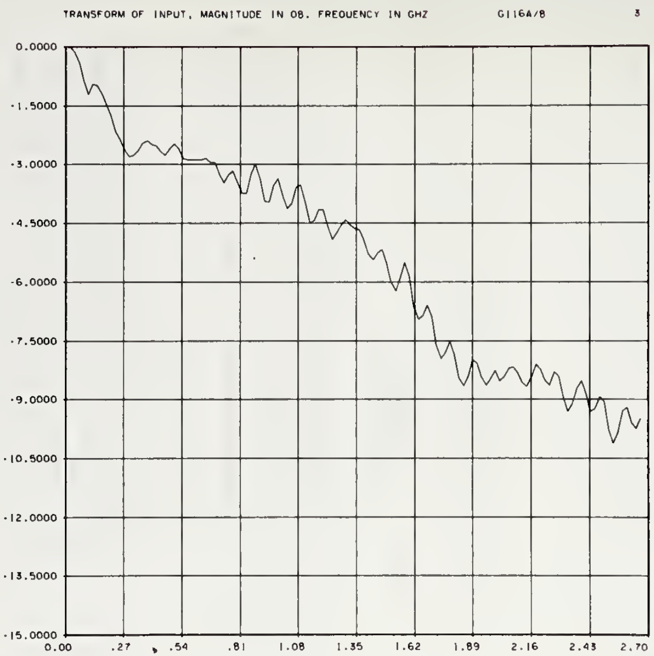

(a)

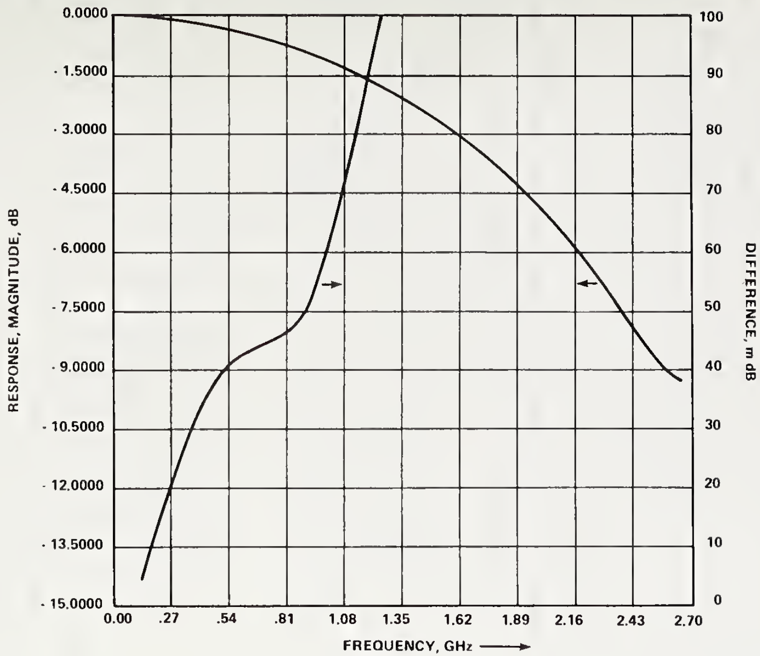

(b)

Figure 4-3. (a) Transform of input pulse out to 2.7 GHz using 50 ns sweep and 256 point FFT. (b) Estimation of aliasing error, left ordinate is FFT of a Gaussian having the same 10 dB frequency as (a) and the same sampling parameters, right ordinate is difference between FFT and exact, analytically computed transform.

difference between that magnitude and an analytically computed transform. At frequencies below about 1250 MHz the difference is less than about 0.1 dB. At frequencies below 800 MHz where these sampling parameters are used, the maximum difference is 0.045 dB, which is within the observed precision of the complete system. Some caution in interpreting these numbers is necessary, however, because the shape of the transform is different in the two cases.

One approach to decreasing the aliasing error without decreasing the resolution or requiring excessive measurement time is to artificially extend the baseline. One might, for example, take 256 samples over about 10 ns and artificially extend the data to include 1024 points over 40 ns. The aliasing error would be substantially reduced while the resolution would be only about 20% worse. This aproach has not yet been used in this system because of uncertainty in the procedure for creating the simulated data, in particular, because the low frequency part of the transform is strongly dependent on the data in the baseline.

Another concern is the manner in which the transforms are scaled. The zero frequency point has no meaning in this system since dc levels in the data are arbitrary. One choice is to reference the entire transform to the first point in the frequency domain. Thus, it is important to maintain good frequency resolution, even for high bandwidth fibers because any variation between zero frequency and the first point is lost. Furthermore, the transform does not necessarily decrease monotonically with frequency, which sometimes can be the case for the first few points in the low frequency range; consequently, the apparent value of the transform can have values greater than unity. Presently, this system normalizes the transforms to the largest value and the interpretation of such effects is left to the user.

5. SYSTEM PERFORMANCE

5.1 Precision

Precision refers to the reproducibility of a measurement. A precision statement, however, says nothing about "systematic" error which is the offset of the average of a large number of measurements from the true value. In the case of optical fibers it is difficult to assign systematic errors since launching condition have yet to be standardized.

Precision is defined here as the reproducibility of the frequency response curve (magnitude). To determine this, measurements were repeated five times on the same fiber. For each measurement the fiber was recleaved and the necessary parts of the measurement system realigned. Three

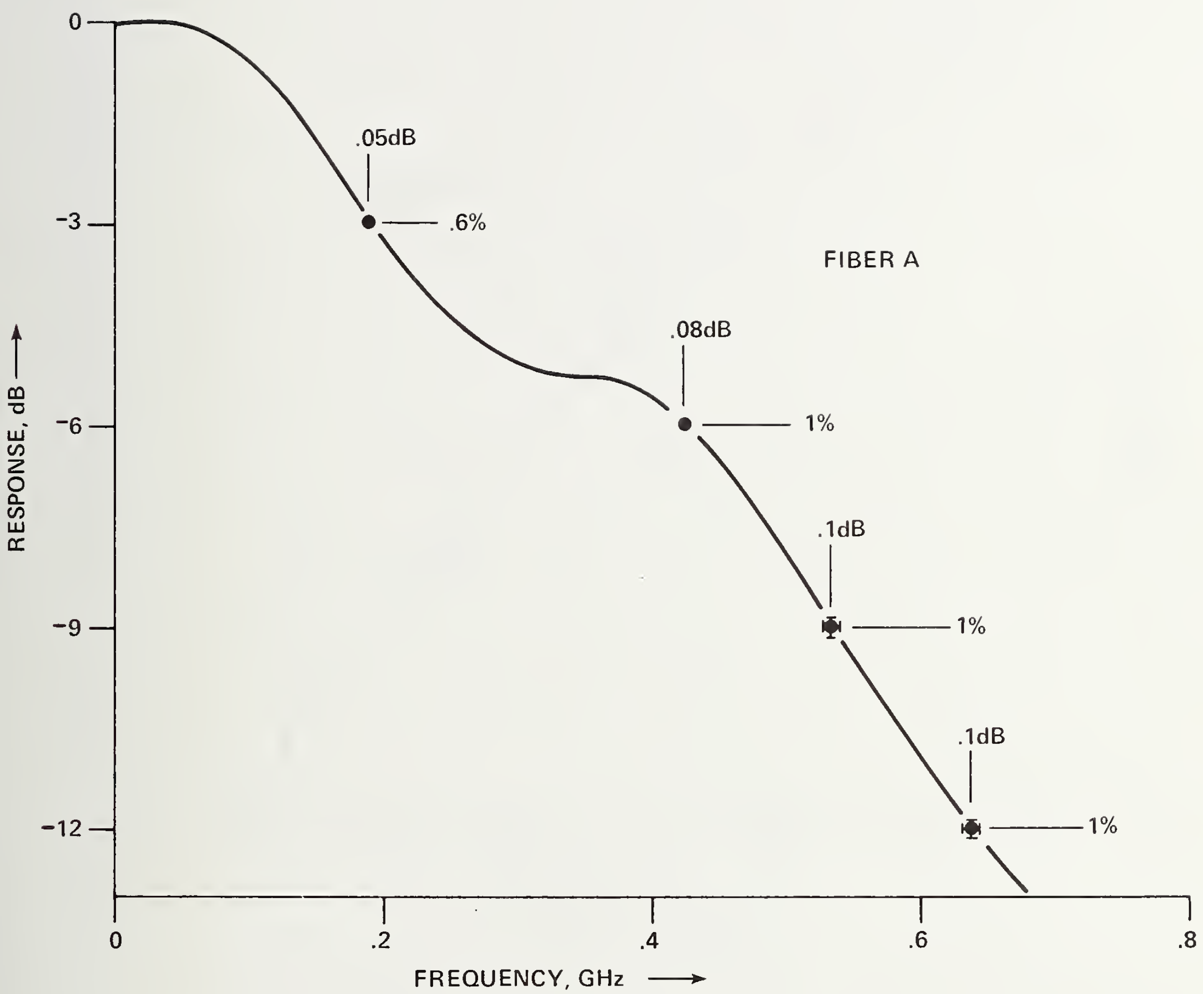

Figure 5-1. System precision, 824 nm diode; error bars are ±1 standard deviation (2 standard deviations in length) for five repeated bandwidth measurements. Fiber A: graded index, 50 μm core, 125 μm O.D., .25 NA, plastic jacketed, 6.0 dB/km attenuation at 850 nm, 1.3 km length.

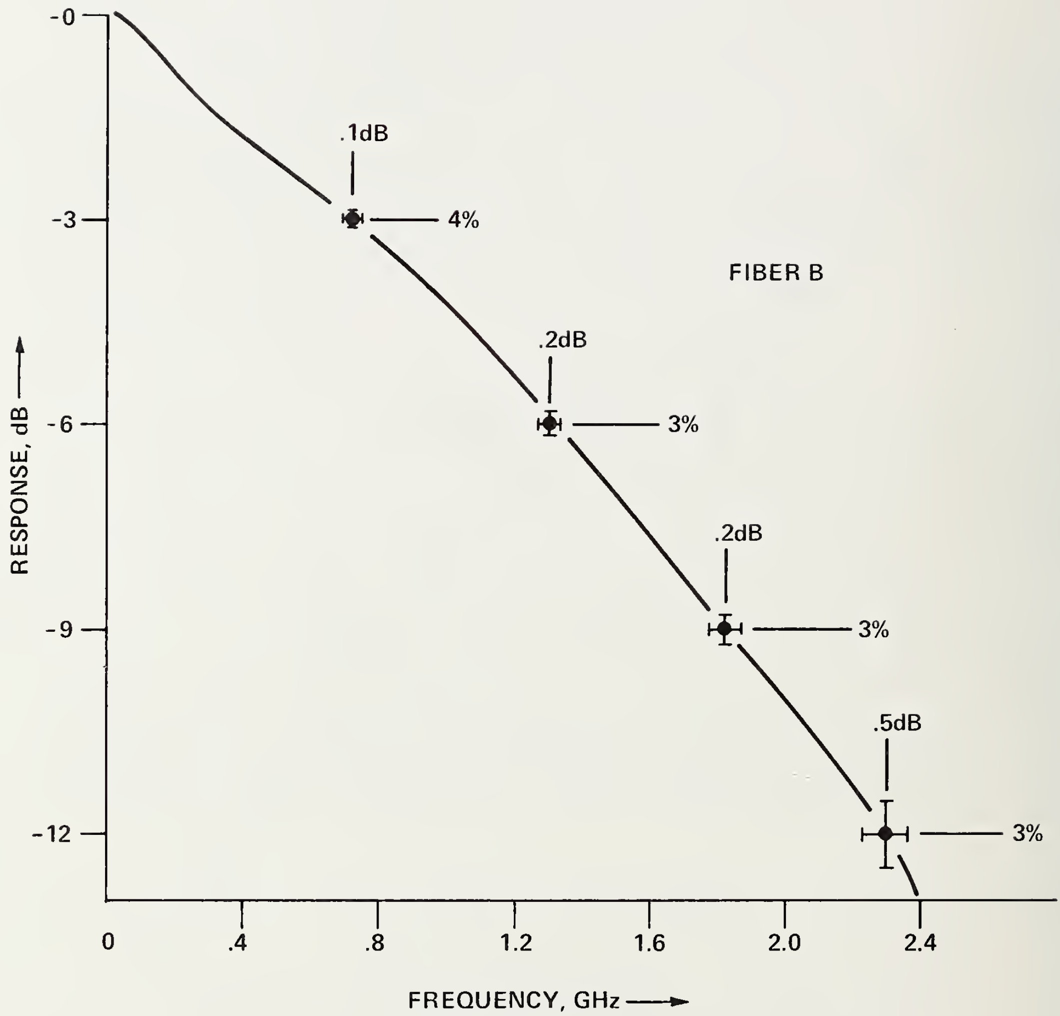

Figure 5-2. System precision, 902 nm diode; error bars are ±1 standard deviation (2 standard deviations in length) for five repeated bandwidth measurements. Fiber B: graded index, 50 μm core, 125 μmO.D., .25 NA plastic jacketed, 4.6 dB/km attenuation at 850 nm, 1.1 km length.

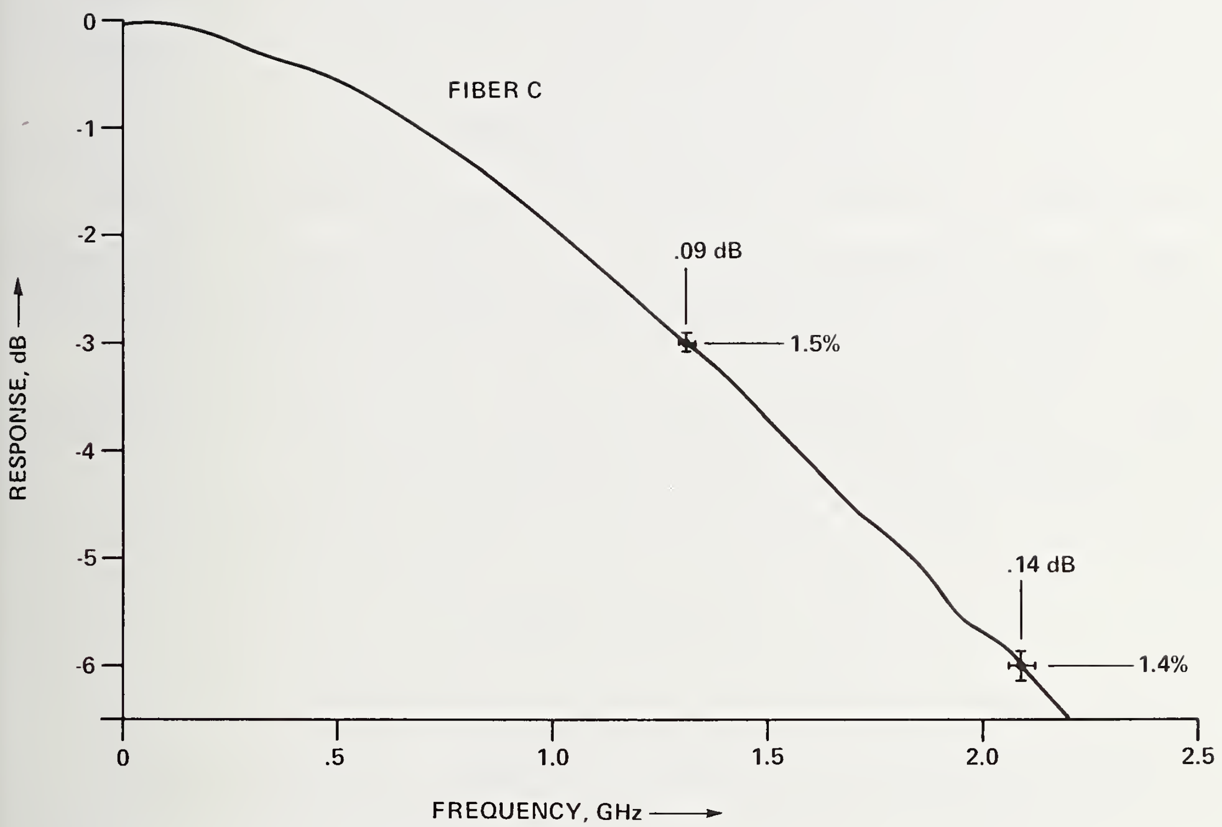

Figure 5-3. System precision, 824 nm diode; error bars are ±1 standard deviation (2 standard deviations in length) for five repeated bandwidth measurements. Fiber C: graded index, 62 μm core, 125 μm O.D., .25 NA, light buffer, 4.0 dB/km attenuation at 850 nm, 1 km length.

multimode, graded index, telecommunications type fibers with a range of bandwidths were chosen for this set of measurements and represent fiber from two different manufacturers. Also, measurements were made using two different laser diodes. The results therefore represent typical system performance.

Results are given in figures 5-1, 5-2, and 5-3 with two-dimensional error bars representing an estimate of ± one standard deviation determined from the five measurements. To summarize the results, error bars are displayed at the 3, 6, 9, and 12 dB points on the frequency response curve. These frequencies were determined by interpolating between discrete FFT points and this precision is indicated by the horizontal error bars. The closest discrete frequencies to the average 3, 6, 9, and 12 dB frequencies were used to determine the precision in the vertical axis. In all cases, a 256 point FFT was used and the time base chosen so that the separation between frequency points was 21 MHz for fiber A and 54 MHz for fibers B and C. In plotting the figures, a smooth curve was drawn through the points.

Some fibers gave better measurement precision than others. Fiber A with the lowest bandwidth (200 MHz) gave the best precision with the frequency at a given response being determined to 1% and the response at a given frequency being determined to .1 dB. For fiber B with medium bandwidth (720 MHz), the corresponding numbers varied from 2 to 4% and .1 to .5 dB with the highest frequency part of the curve showing the poorest reproducibility. Fiber C with the highest bandwidth (1.3 GHz), gave corresponding precisions of 1 to 2% and .1 to .2 dB respectively.

5.2 Dynamic Range

Dynamic range applies to both the maximum fiber bandwidth and attenuation that can be accommodated by the system. If only the intermodal contribution is to be determined from a measurement, the upper bandwidth limit is determined by the spectral properties of the laser diodes and is in the 1-2 GHz·km, 3 dB frequency range depending upon the specific diode. Although higher bandwidths can be measured, the material dispersion contributions become too large and accurate corrections become difficult (section 4.3). Limitations due to source pulse width (260 ps FDHM) do not become important until the 3 dB frequency exceeds 3 GHz.

Maximum attenuation limits depend upon the amount of signal averaging done or on the signal level available to the sampling oscilloscope trigger for good stability. Present sources, attenuated with a 1.0 neutral density filter and detected with a BPW-28 APD (section 3.2), produce from .2 to 2 volts at the detector for short lengths of fiber having negligible attenuation and high bandwidth.

If an advanced trigger-electrical delay line is used with the output signal, figure 3-18(b), we find about 15 mv of signal should be available for the oscilloscope trigger to provide good long term stability. If the trigger level is not a problem, for example, with a digital time delay generator (figure 3-18(a)), then the amount of signal averaging determines the attenuation limits. For the present amount of analogue averaging (section 3.4), the noise level is less than .1 mv. Both the fiber attenuation and bandwidth will determine the peak voltage level available at the detector output. Signal level in the present system has not been a problem for most of the currently available telecommunications type fibers at the 1-1.5 km length.

5.3 Material Dispersion Limits

In characterizing the bandwidth of multimode fibers, it is desirable to know the intermodal contribution. If the measurement contains significant intramodal broadening, the result depends upon the source spectral properties and does not represent the ultimate bandwidth potential of the fiber.

Material dispersion results in intramodal pulse broadening with the RMS contribution to total pulse broadening given by eq (6), section 2. From the observed diode lineshapes and occasional chirping behavior, it seems unlikely that eq (6) could be used to calculate a significant correction term with a high degree of confidence. A more prudent approach would be to place an upper bandwidth limit on measurements made with a particular diode; i.e., for measured fiber bandwidths below a certain maximum 3 dB bandwidth, f_m, the contribution from intramodal effects for a given diode would be less than 6 percent of the measured bandwidth.

Material dispersion constants were measured for a number of commercial fibers with the apparatus described in the Appendix. The results give M (-M plotted) in figure 7-3 where

$$M = -\frac{\lambda}{c}\frac{d^2n}{d\lambda^2} . \qquad (16)$$

Since the M values at a given wavelength show little variation among fibers (a ± 10% variation would nearly bracket the data), the value of f_m determined is, roughly a property of a given diode. Using a Gaussian approximation for spectral, pulse and fiber frequency response shapes along with the M values from Figure 8-3, eq. (5) and (6) predict an f_m of 1.0, 2.0, and 1.4 GHz·km for the 803, 866, and 902 nm diodes respectively. Chirping observed in the 824 nm diode should partially compensate the material dispersion broadening for fibers exceeding a critical length [12]. From the linear chirping theory of [12], a critical length of 1.1 km is predicted. For shorter lengths, pulse compression would occur. For the pulse widths involved (260 ps), and the fiber lengths measured (1 km or more), intramodal broadening effects are negligible for the 824 nm diode if fiber bandwidth is below 1.1 GHz·km.

For a measurement at the bandwidth limit f_m, the six percent correction could be handled in the following manner. Add 8% to the measured bandwidth in the frequency domain and then take a ± 4% error. This allows for nearly a ± 40% uncertainty in determining f_m. Such a generous uncertainty is possible since at f_m the intramodal contribution represents a small correction to the bandwidth.

6. RESULTS OF BANDWIDTH RELATED MEASUREMENTS

The purpose of this section is to demonstrate typical fiber bandwidth behavior in a quantitative manner. Results were selected from about 20 fibers and represent a diverse mix of properties.

6.1 Wavelength Dependence of Bandwidth

Differences in the refractive index dispersion of the constituents used in making graded index optical fibers results in an index profile that is wavelength dependent. This "profile dispersion" directly affects the optical fiber bandwidth which depends critically on the shape of the index profile. Cohen has shown that bandwidth may increase or decrease with wavelength depending upon the profile characteristics [22].

Figure 6-1 shows a 1.6 km fiber with a rather large wavelength dependence in the bandwidth. Figure 6-1(a) gives the output at 803 nm while figure 6-1(b) is the output at 902 nm. The inputs were 330 ps FDHM for both wavelengths. Measurements of the transfer functions indicated the 3 dB bandwidth decreased from 0.90 GHz·km at 803 nm to 0.61 GHz·km at 902 nm.

6.2 Mode Mixing

In a multimode optical fiber, power can be coupled between modes as a result of perturbations in the optical characteristics induced by physical changes. If fast and slow modes are mixed, the delay times tend to be equalized and the bandwidth increases. Figure 6.2(a) shows the output of a 1

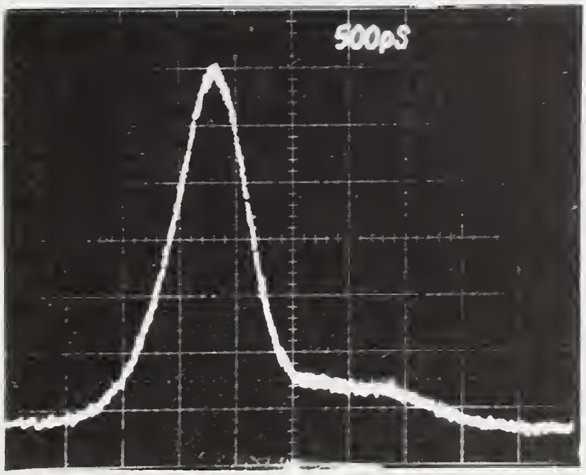

OUTPUT PULSE
803 nm

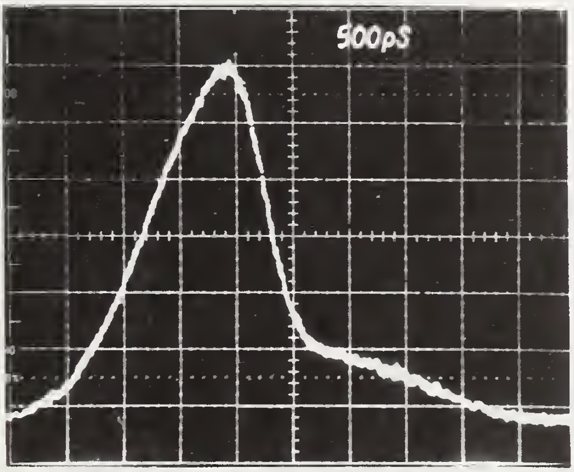

OUTPUT PULSE
902 nm

Figure 6-1. Output pulses from 1.5 km, graded index optical fiber at two wavelengths, (a) 803 nm, (b) 902 nm for nearly identical shaped input pulses of 330 ps FDHM..

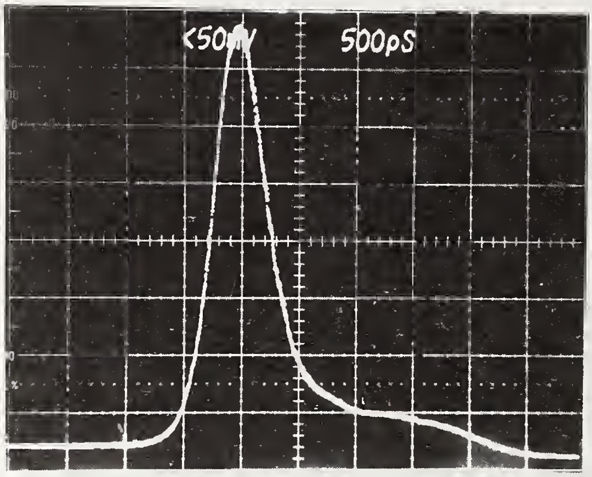

(a)

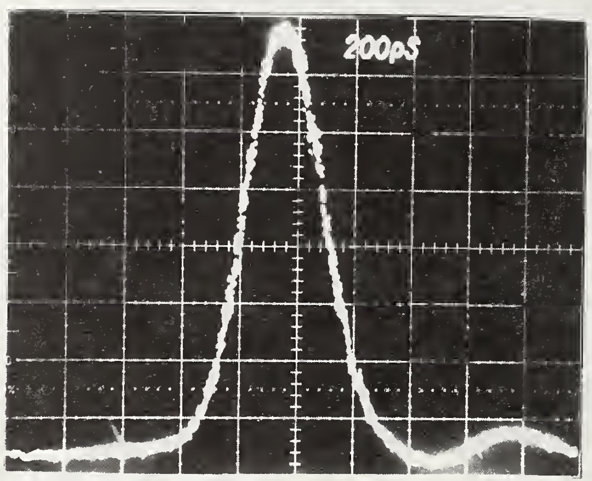

(b)

Figure 6-2. Influence of microbending on bandwidth of a lightly buffered graded index optical fiber, 1 km length, (a) output pulse with fiber wound loose in a single layer, (b) output pulse with fiber wound under stress in multiple layers (824 nm diode). In (b) the output pulse shape is barely distinguishable from the input; due to microbending bandwidth has been increased by approximately a factor of four.

km lightly buffered fiber, loosely wound in a single layer on a measurement spool. The input pulse duration was about 300 ps. Figure 6.2(b) shows the output using the same source but now with the fiber under tension and wound in multiple layers so as to introduce microbending. The bandwidth has now increased so that the output pulse is barely distinguishable from the input and is largely representative of the intramodal broadening occuring in the fiber. Fiber attenuation also increased between these two cases; an additional microbending loss of more than 10 dB was incurred to achieve the above bandwidth enhancement.

6.3. Accuracy of Gaussian Predictions

If the fiber frequency response and input pulse are assumed to be Gaussian, the 3 dB bandwidth may be predicted by a simple deconvolution of the input pulse duration from the output pulse duration (section 2. eq. (11)). The accuracy of this assumption was checked using the present system to measure the actual bandwidth. All fibers measured over a given period of time with the system are included with no preselection. Output pulse shapes ranged from symmetric to assymmetric (usually the latter), some with long leading edges others with long trailing edges; however, none of the pulses exhibited multiple peaks. The results are given Table IV. The agreement is close enough for some purposes and is in accord with similar statements made by Midwinter [23].

6.4 Fiber Response Pathologies

The impulse response - transfer function characteristics of multimode fibers show a rich variability. The purpose of this section is to demonstrate the range of behavior that can be observed.

6.4.1 Pulse Shapes

In some cases, output waveforms from multimode fibers exhibit multiple pulses or peaks. Results similar to those reported by Eickhoff have been observed where energy is carried in an on-axis index peak and for a 1 km fiber arrives over 10 ns later than the main pulse [24]. In another instance, we measured a fiber having 20 multiple peaks resolved to the half-widths in its impulse response. In most situations, however, the fiber response has a single maximum which is frequently assymmetric about the peak. The assymmetry is characterized by either a low level leading edge or a low level trailing edge; this results from an index profile which does not adequately equalize mode arrival time. Figure 6-3 is typical of this

TABLE IV

Accuracy of Gaussian Assumption for Determining 3 dB Bandwidth from Half-Duration Pulse Broadening

Graded Index Fiber	Length, km	Bandwidth, Gaussian Prediction, MHz	Actual Bandwidth, MHz	Percentage Difference, %
308	1.4	256	198	+ 29%
223	1.1	846	732	+ 16%
116	1.6	612	673	- 9%
206	1.0	713	752	- 5%
1206	1.4	280	325	- 14%
1208	1.4	189	210	- 10%
1212	.7	467	402	+ 16%
207	1.0	1048	1062	- 1%
156	1.0	164	184	- 11%

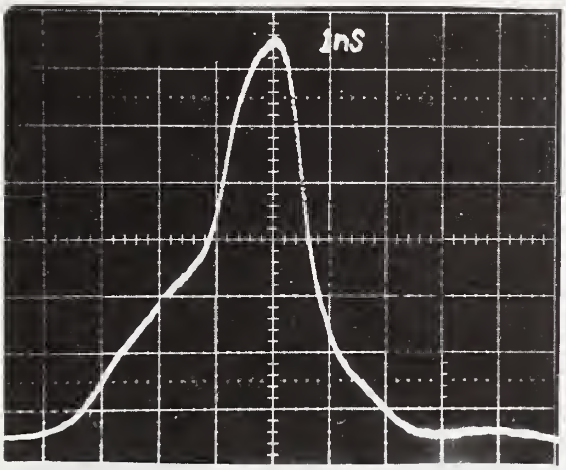

(a)

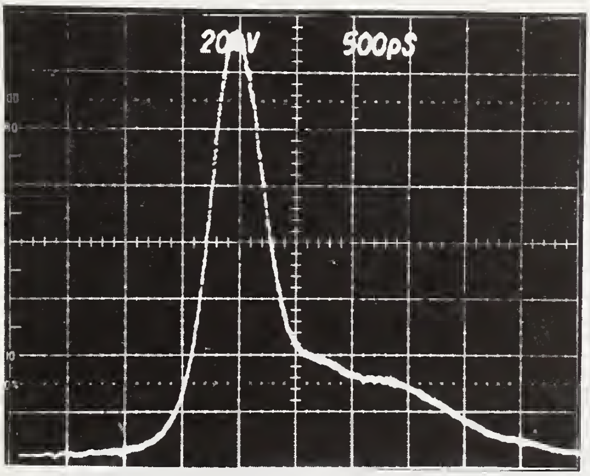

(b)

Figure 6-3. Opposite pulse broadening behavior in graded index optical fibers, (a) 1.1 km fiber (fiber B, 902 nm) with some modes arriving too early, (b) 1.3 km fiber (fiber A, 824 nm) with some modes arriving too late.

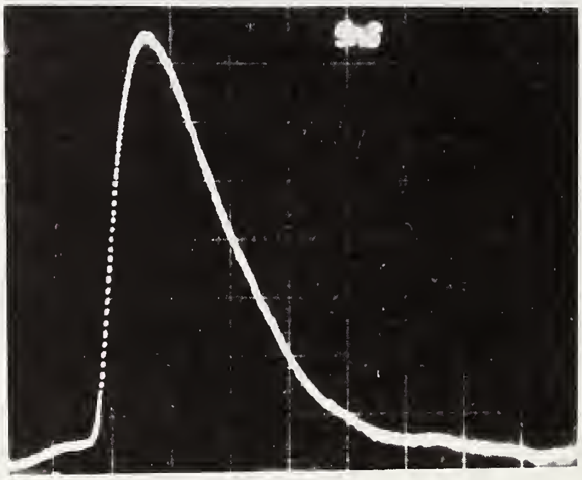

(a)

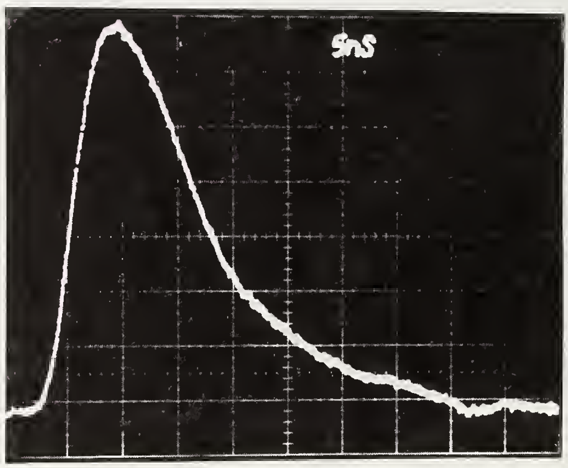

(b)

Figure 6-4. Characteristic impulse response for step index fibers (a) 85 μm core, .18 NA, .8 km length, 824 nm and (b) 55 μm core, .25 NA, 1.2 km length, 824 nm.

behavior. If one assumes most of the energy is carried in low to medium order modes, then the fiber in figure 6-3(a) represents a profile with insufficient doping near the cladding (high order modes arrive too early and are overcompensated with respect to group velocity) while the opposite (too much doping and undercompensation) would be true in figure 6-3(b).

While graded index fibers exhibit great variations in behavior, multimode step fibers have a characteristic impulse response. The impulse response has a rapid rise with a nearly ramp-like decay lasting for a longer time (figure 6.4). This general behavior is roughly predicted by simple mode propagation models [25].

6.4.2 Frequency-Phase Characteristics

Since output pulses from fibers show diverse behavior, it is not surprising that the frequency response characteristics also exhibit a diversity. This is evident in a comparison of the magnitude and phase responses for fibers. Fibers have been observed where the significant distortion in the phase has occurred both before and after the frequency where the magnitude is down by 3 dB. Examples of both kinds of behavior are given in figures 6-5 and 6-6. No distortion in the phase is represented by a straight line on these plots; i.e., linear phase shift with frequency. For the fiber of figure 6-5, the phase distorts significantly before the 3 dB frequency; while in figure 6-6, the phase is fairly linear out to the 5 dB frequency.

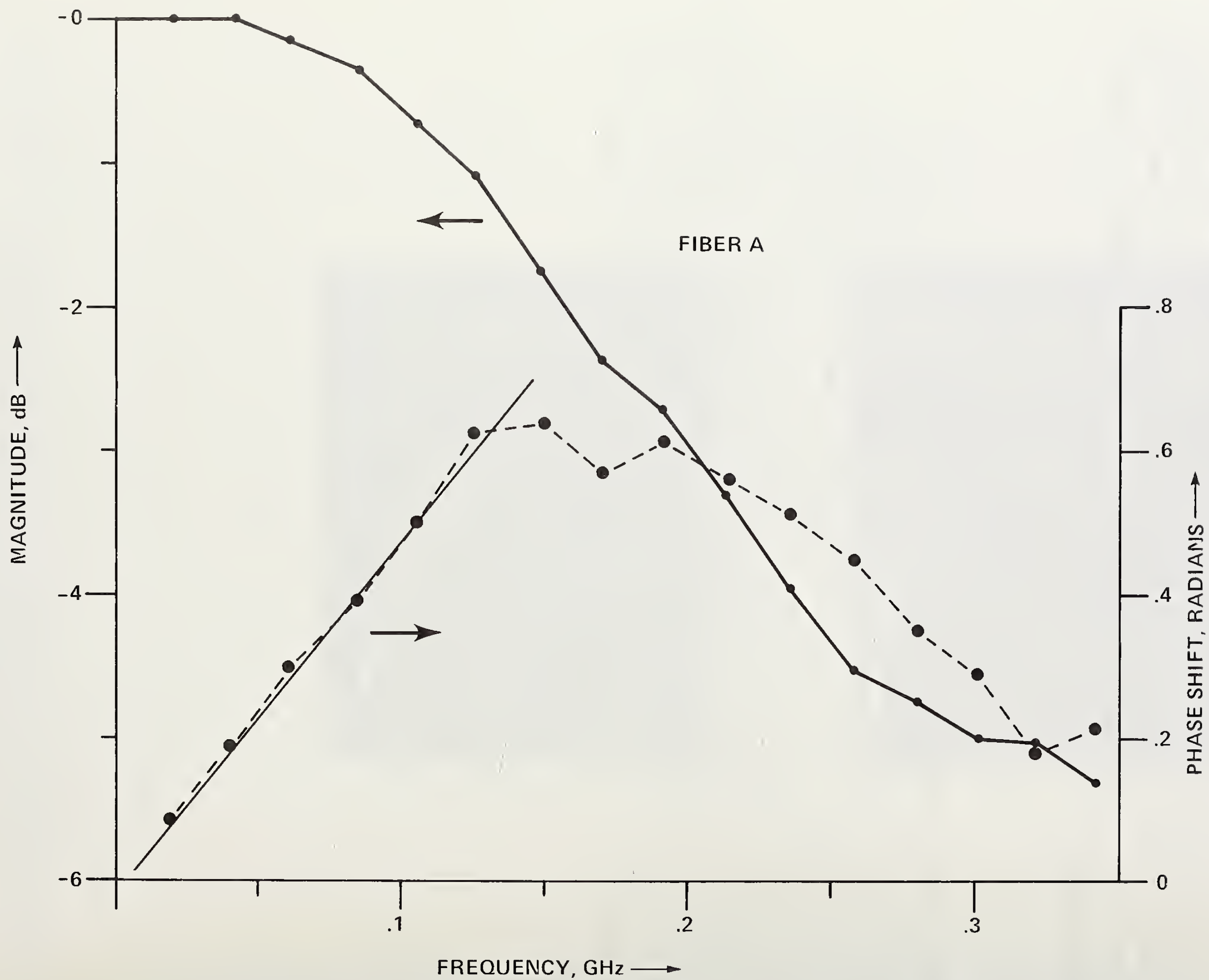

Figure 6-5. Magnitude and phase of the transfer function versus frequency for a graded index fiber exhibiting large phase distortion (Fiber A, 1.3 km length, 824 nm).

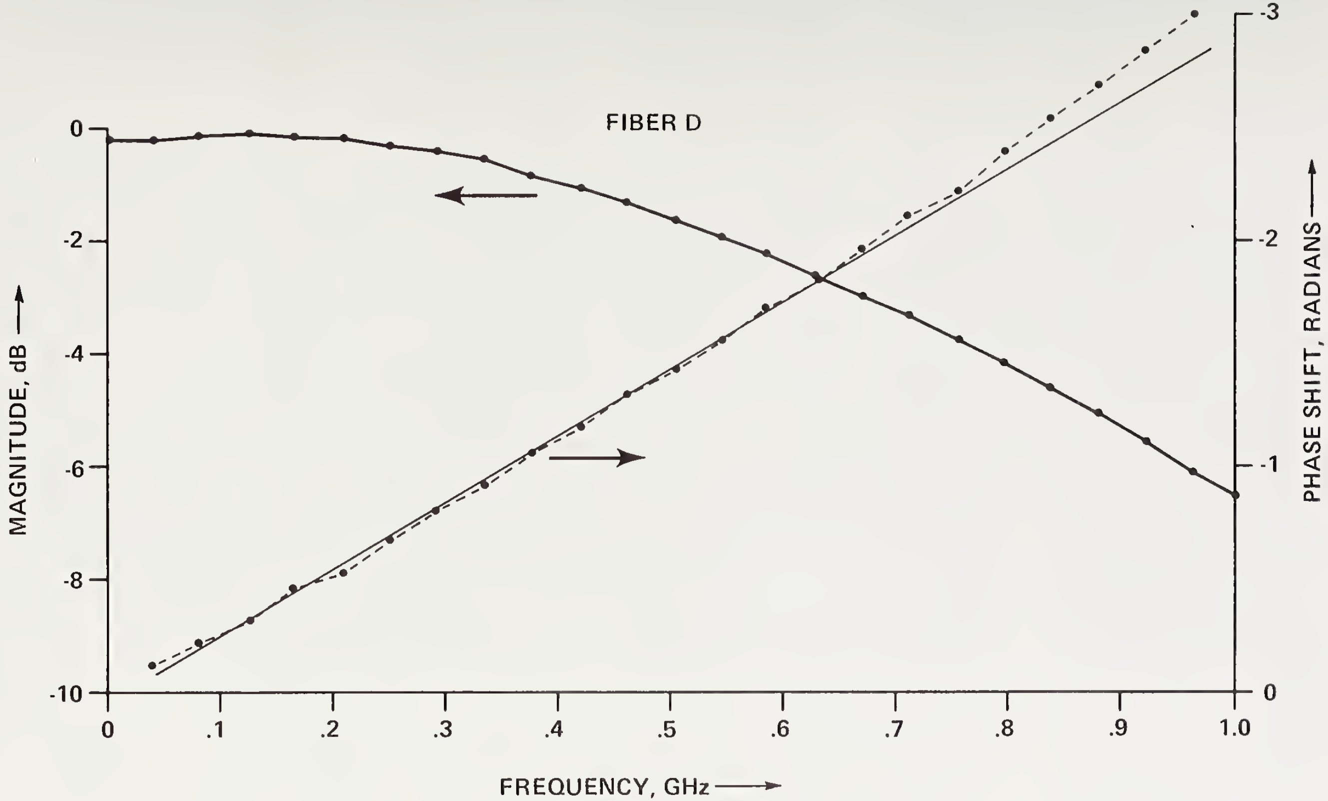

Figure 6-6. Magnitude and phase of the transfer function versus frequency for a graded index fiber exhibiting low phase distortion (Fiber D, 1.5 km length, 824 nm).

7. CONCLUSIONS

Perhaps the greatest uncertainty in making bandwidth measurements on multimode fibers is the lack of standardized launching conditions. This makes a discussion of systematic error difficult because at the present one cannot say that one launching condition is more "correct" than another. The launching conditions presently employed with this system tend to over fill the fiber under test. A spot size of 55 μm and a launch NA of .25 will fill the mode volume of most fibers meeting the proposed standard core size of 50 μm. Such a launching condition has the following merits. 1) It will give a lower estimate to the bandwidth encountered in actual systems and therefore could be used in "worst case" calculations. 2) It is the starting point for the use of equilibrium mode simulators (EMS). An EMS would strip away specific high loss modes which do not propagate very far in the fiber. 3) It can be reproduced by other laboratories and is independent of a particular diode radiation characteristic.

Some additional work needs to be done by standards groups on the terminology used in reporting bandwidth. For multimode fibers, reporting the intermodal contribution seems appropriate. The intramodal part could be specified as a function of wavelength by the manufacturer based on refractive index data and specified per unit fiber length and source linewidth. Also, a problem remains on reporting the bandwidth per unit length where the actual measurement length is quite different from the unit length.

With improved fiber characteristics at the longer wavelengths, more emphasis will be placed on bandwidth measurements over the 1.1 - 1.5 μm region. Many of the points emphasied in this Technical Note still remain valid. Material dispersion however will not be as important since the material broadening is approximately 40 ps/km.nm at 1.1 μm and even less for longer wavelength.

8. APPENDIX

This appendix describes measurements of optical fiber material dispersion constants. Material dispersion was measured by a technique described by Gloge et al. [26]. In this method, the dispersion is determined by noting the differential delay between pulses from two different wavelength laser diodes. This work utilizes the same method with the following extensions: (1) four laser diodes with appropriate wavelengths to cover the whole 0.8 - to 0.9-micrometer wavelength region, (2) shorter pulse widths to provide good resolution, (3) a mode scrambler to reduce effects of differential launching conditions, and (4) the use of high-bandwidth fibers to minimize intermodal contributions.

An experimental configuration for determining material dispersion is shown in figure 8-1. By pulsing pairs of diodes, pulses at two different wavelengths were launched down the test fiber. Diodes at 803, 824, 866, and 902 nm were used to cover the 0.8- to 0.9-micrometer region. Pulses were separated slightly in time before launching to avoid overlap which would shift the positions of the peaks. A pulse pair before and after traversing a 1-km fiber length is shown in figure 8-2(a) and (b). In this case, a wavelength difference of 21 nm gives a differential delay of 2.4 ns. Measurements of differential delay between pulses were repeatable within ± 100 ps.

Material dispersion was determined for fibers labeled 2, 4, and 5, figure 8-3. These fibers had lengths of 1.0, 1.5, and 1.4 km and exhibited pulse FDHM broadenings of .42, .74, and 1.1 ns, respectively. Bandwidth (3 dB optical) determined in the frequency domain by the fast Fourier transform (FFT) ratio of output to input pulses was 1.1, 0.9, and 0.4 GHz-km, respectively. A single point, A, inferred from the data of [26] is also shown in figure 8-3. Other data from the literature representing fibers measured at CSELT using similar techniques is included (curve C) [27]. Overall, results do indicate significant, measureable differences between fibers. However, at any one wavelength, a ± 10 percent variation would nearly bracket the data. The result on fiber 2 has the least influence from intermodal delay of the fibers measured. This fiber exhibited the highest bandwidth and the least variation of bandwidth with wavelength. Also, the manufacturer of fiber 2 provided sufficient, representative index data to determine eq. (16), at 800, 850, and 900 nm. Values of M from this data are indicated by the dashed curve and are slightly above the experimental values. While the above measurements were limited to the 800-900 nm wavelength region, other experimental results are available from the literature for longer wavelengths [28], [29].

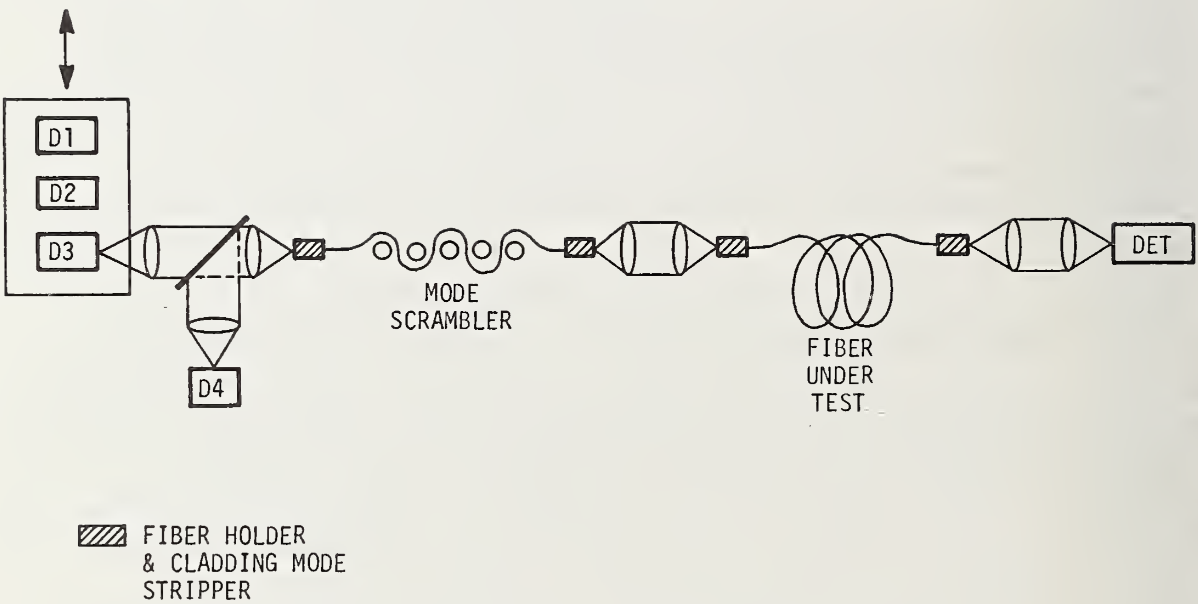

Figure 8-1. Apparatus for measuring material dispersion by simultaneous propagation of pulses from pairs of laser diodes.

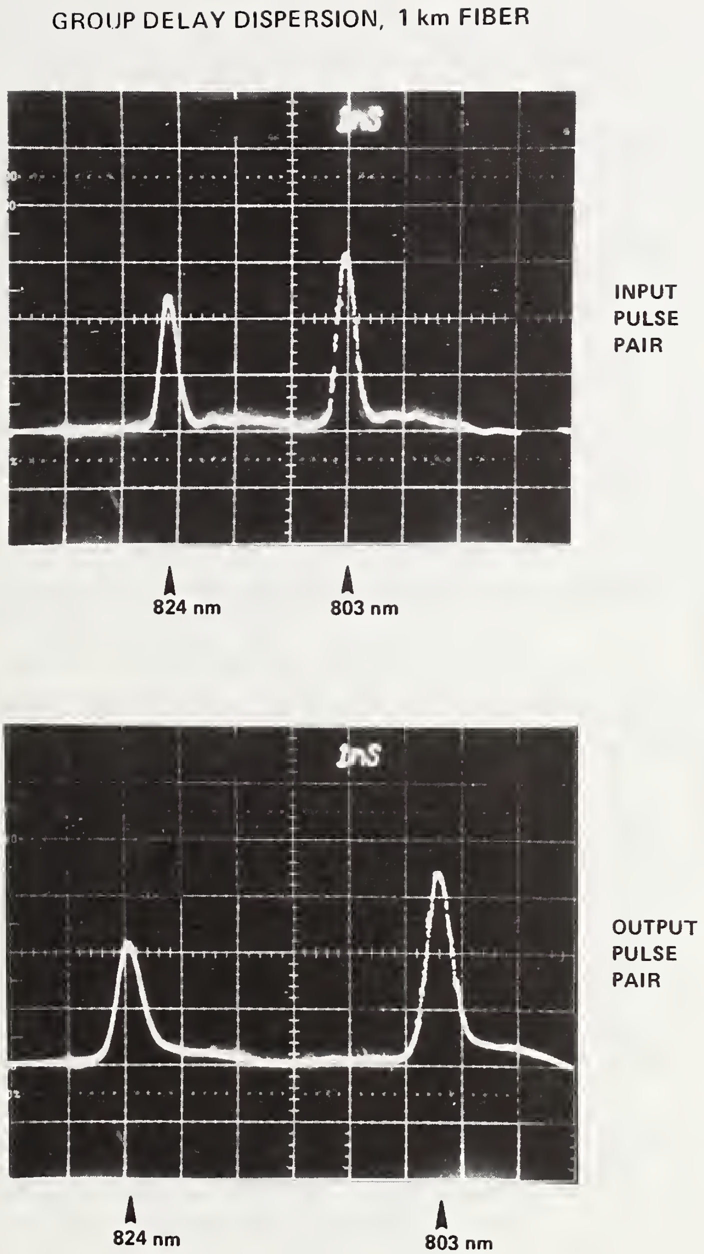

Figure 8-2. Example of material dispersion in an optical fiber showing a pulse pair (a) before and (b) after propagating through a 1 km length of fiber.

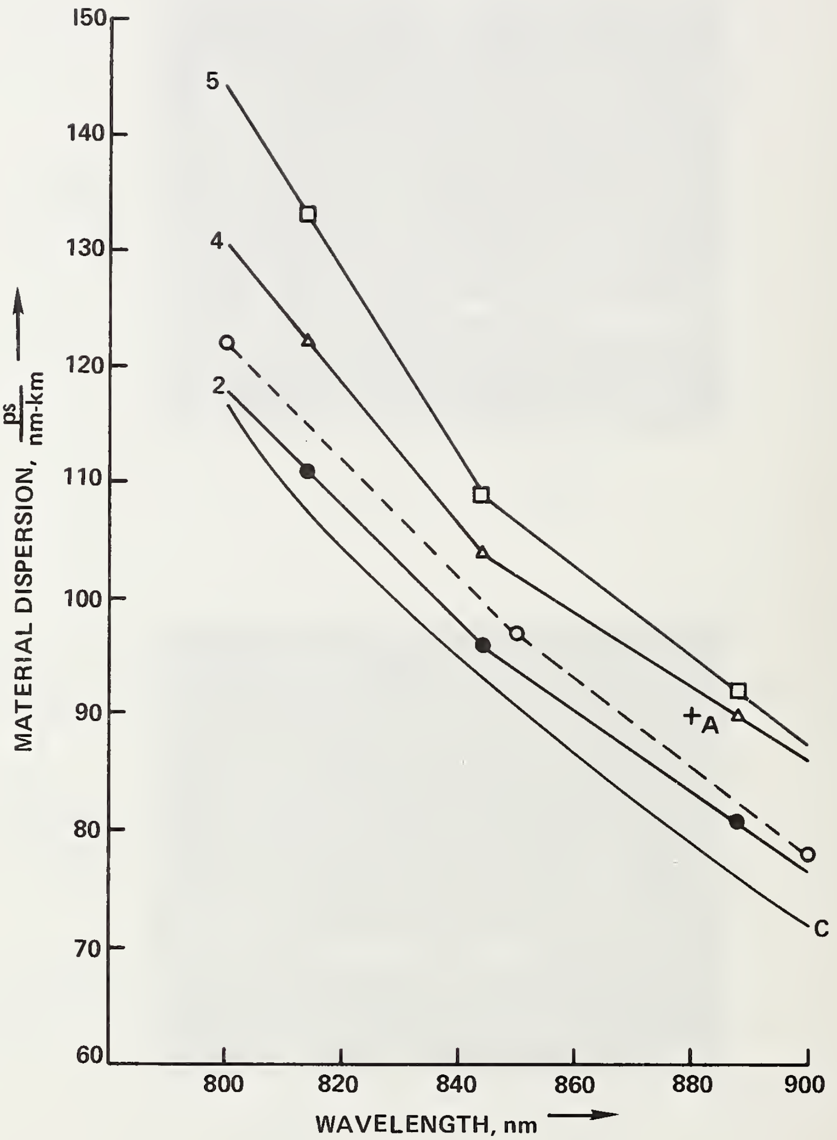

Figure 8-3. Material dispersion constants for a number of commercially available graded index fibers labeled 2, 4, and 5. Curve C and point A are measurements from the literature while the dashed curve is calculated from index data supplied by the manufacturer of fiber 2.

9. REFERENCES

[1] Olshansky, R. and Keck, D. B., Pulse broadening in graded-index optical fibers, Applied Optics, 15, No. 2, 483-491 (Feb. 1976).

[2] Cohen, L. G., Shuttle pulse measurements of pulse spreading in an optical fiber, Applied Optics, 14, No. 6, 1351-1356 (June 1976).

[3] Cohen, L. G., Astle, H. W., and Kaminow, I. P., Frequency domain measurements of dispersion in multimode optical fibers, A.P.L., 30, No. 1, 17-19 (Jan. 1, 1977).

[4] Vassallo, Linear power responses of an optical fiber, IEEE Transactions on Microwave Theory and Techniques, MTT-25, No. 7, 572-576 (July 1977).

[5] Machida, S., et al, Interference of an AlGaAs laser diode using a 4.15 km single mode fiber cable, IEEE Journal of Quantum Electronics, QE-15, No. 7, 535-537 (July 1979).

[6] Gloge, D., Chinnock, E. L., and Lee, T. P., Self-pulsing GaAs laser for fiber-dispersion measurements, IEEE Journal of Quantum Electronics, QE-8, No. 11, 844-846 (Nov. 1972).

[7] Keck, D. B., Spatial and temporal power transfer measurements on a low-loss optical waveguide, Applied Optics, 13, 1882-1888 (Aug. 1974).

[8] Hansen, J. B. and Schmidt, W. A., A fast risetime avalanche transistor pulse generator for driving injection lasers, Proc. IEEE, 55, No. 2, 216-217 (Feb. 1967).

[9] Andrews, J. R., Inexpensive laser diode pulse generator for optical waveguide studies, Rev. Sci. Instrum., 45, No. 1, 22-24 (Jan., 1974).

[10] Dannwolf, J. W., et al, Optical-Fiber impulse-response measurement system, IEEE Transactions on Instrumentation and Measurement, IM-25, No. 4, 401-406 (Dec. 1976).

[11] In order to describe adequately the experimental procedure and permit reproduction of this work, certain commercial components are mentioned here and elsewhere; in no way does this represent an endorsement by NBS. Other components may work equally well or better.

[12] Wright, J. V. and Nelson, B. D., Pulse compression in optical fibers, Electronics Letters, 13, No. 12, 361-363 (June 1977).

[13] Green, S. I., 50 picosecond detector pulse monitor, Rev. Sci. Instrum. 47, No. 9, 1083-1085 (Sept. 1976).

[14] The authors would like to thank Matt Young of the Time-Domain Metrology Section of NBS for use of his mode-locked Nd:YAG laser.

[15] Costa, B., et al, Wavelength dependence of differential group delay in graded-index optical fibers: application to fiber-links characterization, paper ThG5, Topical Meeting on Optical Fiber Communications, March 6-8, 1979, Washington, D.C.

[16] Green, S. I., Wideband 1.064 micrometer detector evaluation, McDonnell Douglas Astronautics Co. Final Report NA55-20616 (NTIS # N77-32459/8wz).

[17] Love, W. F., Novel mode scrambler for use in optical-fiber bandwidth measurements, paper ThG2 Topical Meeting on Optical Fiber Communications, March 6-8, 1979, Washington, D.C.

[18] Tokuda, M., et al, Measurement of baseband frequency response of multimode fibre by using a new type of mode scrambler, Electronic Letters, 13, No. 5, 146-147 (March 3, 1977).

[19] Dakin, J. P., et al, Launching into glass fibre optical waveguides, Optical Communications, 4, No. 5, 354-357 (Jan. 1972).

[20] Andrews, J. R., and Young, M., Time domain measurements on optical communications components, NBSIR - to be published.

[21] Ramirez, R. W., Evaluating fibers digitally, Laser Focus, 15, No. 4, 46-52 (April 1979).

[22] Cohen, L. G., et al, Profile dispersion effects on transmission bandwidths in graded index optical fibers, IEEE J. Quantum Electronics, QE-14, No. 1, 37-41 (Jan. 1978).

[23] Midwinter, J. E., Optical Fibers for Transmission, John Wiley & Sons, New York, N.Y. (1979).

[24] Eickhoff, W. and Krumpholtz, O., Pulse response and microbending losses of an optical glass-fibre waveguide with a bump in its index profile, Electronics Letters, 13, No. 9, 256-257 (April 1977).

[25] Gallawa, R. L., A User's Manual for Optical Waveguide Communications, NTIA, Report #OTR 76-83.

[26] Gloge, D., Chinnok, E. L., and Lee, T. P., GaAs twin-laser setup to measure mode and material dispersion in optical fibers, Applied Optics, 13, No. 2, 261-263 (Feb. 1974).

[27] Sordo, B. Esposto, F., and Costa, B., Proceedings of the Fourth European Conference on Optical Communications, Genova, Italy, Sept. 12-15, 1978.

[28] Payne, D.N., and Hartog, A.H., Determination of the wavelength of zero material dispersion in optical fibers by pulse-delay measurements, Electron. Lett., 13, No. 21, 627-629 (Oct. 1977).

[29] Cohen, L.G., and Chinlon, L., Pulse delay measurements in the zero material dispersion wavelength region for optical fibers, Applied Optics, 16, No. 12, 3136-3139 (Dec. 1977).

☆U.S. GOVERNMENT PRINTING OFFICE: 1980—677-096/1232

NBS-114A (REV. 9-78)

U.S. DEPT. OF COMM. BIBLIOGRAPHIC DATA SHEET	1. PUBLICATION OR REPORT NO.	2. Gov't. Accession No.	3. Recipient's Accession No.
	NBS TN-1019		

4. TITLE AND SUBTITLE

Measurement of Optical Fiber Bandwidth in the Time Domain

5. Publication Date

February 1980

6. Performing Organization Code

7. AUTHOR(S)

Douglas L. Franzen and G. W. Day

8. Performing Organ. Report No.

9. PERFORMING ORGANIZATION NAME AND ADDRESS

NATIONAL BUREAU OF STANDARDS
DEPARTMENT OF COMMERCE
WASHINGTON, DC 20234

10. Project/Task/Work Unit No.

11. Contract/Grant No.

12. SPONSORING ORGANIZATION NAME AND COMPLETE ADDRESS *(Street, City, State, ZIP)*

Supported in part by the Department of Defense, Calibration Coordination Group (CCG).

13. Type of Report & Period Covere[d]

14. Sponsoring Agency Code

15. SUPPLEMENTARY NOTES

☐ Document describes a computer program; SF-185, FIPS Software Summary, is attached.

16. ABSTRACT *(A 200-word or less factual summary of most significant information. If document includes a significant bibliography or literature survey, mention it here.)*

A system is described for determining optical fiber bandwidth from time domain information. A measurement gives the optical fiber transfer function (or frequency response) relating the output waveform to the input. An analysis is given of the variables affecting the measurement. This includes a discussion of such input related topics as launching conditions, mode scramblers, and laser diode sources; output related topics include a discussion of optical detectors. Laser diodes are evaluated with respect to short pulse performance, near field emission, material dispersion limits, and other spectral behavior like chirping; detectors are evaluated with respect to time response, linearity, and uniformity. Overall system architecture, precision, and dynamic range are discussed. A number of bandwidth related topics are briefly presented and typical experimental results given. This includes examples of: mode mixing via microbending, profile compensation, profile dispersion, intramodal broadening, materials dispersion cons[...] relative magnitude-phase behavior, and Gaussian predictions of frequency response.

17. KEY WORDS *(six to twelve entries; alphabetical order; capitalize only the first letter of the first key word unless a proper name; separated by semicolons)*

Bandwidth; laser diodes; material dispersion; mode scramblers; optical detectors; optical fibers; transfer function.

18. AVAILABILITY ☒ Unlimited

☐ For Official Distribution. Do Not Release to NTIS

☐ Order From Sup. of Doc., U.S. Government Printing Office, Washington, DC 20402, SD Stock No. SN003-003- 02161-0

☐ Order From National Technical Information Service (NTIS), Springfield, VA. 22161

19. SECURITY CLASS (THIS REPORT)	21. NO. OF PRINTED PAG[ES]
UNCLASSIFIED	72
20. SECURITY CLASS (THIS PAGE)	**22. Price**
UNCLASSIFIED	$3.75

NBS TECHNICAL PUBLICATIONS

PERIODICALS

JOURNAL OF RESEARCH—The Journal of Research of the National Bureau of Standards reports NBS research and development in those disciplines of the physical and engineering sciences in which the Bureau is active. These include physics, chemistry, engineering, mathematics, and computer sciences. Papers cover a broad range of subjects, with major emphasis on measurement methodology and the basic technology underlying standardization. Also included from time to time are survey articles on topics closely related to the Bureau's technical and scientific programs. As a special service to subscribers each issue contains complete citations to all recent Bureau publications in both NBS and non-NBS media. Issued six times a year. Annual subscription: domestic $17; foreign $21.25. Single copy, $3 domestic; $3.75 foreign.

NOTE: The Journal was formerly published in two sections: Section A "Physics and Chemistry" and Section B "Mathematical Sciences."

DIMENSIONS/NBS—This monthly magazine is published to inform scientists, engineers, business and industry leaders, teachers, students, and consumers of the latest advances in science and technology, with primary emphasis on work at NBS. The magazine highlights and reviews such issues as energy research, fire protection, building technology, metric conversion, pollution abatement, health and safety, and consumer product performance. In addition, it reports the results of Bureau programs in measurement standards and techniques, properties of matter and materials, engineering standards and services, instrumentation, and automatic data processing. Annual subscription: domestic $11; foreign $13.75.

NONPERIODICALS

Monographs—Major contributions to the technical literature on various subjects related to the Bureau's scientific and technical activities.

Handbooks—Recommended codes of engineering and industrial practice (including safety codes) developed in cooperation with interested industries, professional organizations, and regulatory bodies.

Special Publications—Include proceedings of conferences sponsored by NBS, NBS annual reports, and other special publications appropriate to this grouping such as wall charts, pocket cards, and bibliographies.

Applied Mathematics Series—Mathematical tables, manuals, and studies of special interest to physicists, engineers, chemists, biologists, mathematicians, computer programmers, and others engaged in scientific and technical work.

National Standard Reference Data Series—Provides quantitative data on the physical and chemical properties of materials, compiled from the world's literature and critically evaluated. Developed under a worldwide program coordinated by NBS under the authority of the National Standard Data Act (Public Law 90-396).

NOTE: The principal publication outlet for the foregoing data is the Journal of Physical and Chemical Reference Data (JPCRD) published quarterly for NBS by the American Chemical Society (ACS) and the American Institute of Physics (AIP). Subscriptions, reprints, and supplements available from ACS, 1155 Sixteenth St., NW, Washington, DC 20056.

Building Science Series—Disseminates technical information developed at the Bureau on building materials, components, systems, and whole structures. The series presents research results, test methods, and performance criteria related to the structural and environmental functions and the durability and safety characteristics of building elements and systems.

Technical Notes—Studies or reports which are complete in themselves but restrictive in their treatment of a subject. Analogous to monographs but not so comprehensive in scope or definitive in treatment of the subject area. Often serve as a vehicle for final reports of work performed at NBS under the sponsorship of other government agencies.

Voluntary Product Standards—Developed under procedures published by the Department of Commerce in Part 10, Title 15, of the Code of Federal Regulations. The standards establish nationally recognized requirements for products, and provide all concerned interests with a basis for common understanding of the characteristics of the products. NBS administers this program as a supplement to the activities of the private sector standardizing organizations.

Consumer Information Series—Practical information, based on NBS research and experience, covering areas of interest to the consumer. Easily understandable language and illustrations provide useful background knowledge for shopping in today's technological marketplace.

Order the **above** *NBS publications from: Superintendent of Documents, Government Printing Office, Washington, DC 20402.*

Order the **following** *NBS publications—FIPS and NBSIR's—from the National Technical Information Services, Springfield, VA 22161.*

Federal Information Processing Standards Publications (FIPS PUB)—Publications in this series collectively constitute the Federal Information Processing Standards Register. The Register serves as the official source of information in the Federal Government regarding standards issued by NBS pursuant to the Federal Property and Administrative Services Act of 1949 as amended, Public Law 89-306 (79 Stat. 1127), and as implemented by Executive Order 11717 (38 FR 12315, dated May 11, 1973) and Part 6 of Title 15 CFR (Code of Federal Regulations).

NBS Interagency Reports (NBSIR)—A special series of interim or final reports on work performed by NBS for outside sponsors (both government and non-government). In general, initial distribution is handled by the sponsor; public distribution is by the National Technical Information Services, Springfield, VA 22161, in paper copy or microfiche form.

BIBLIOGRAPHIC SUBSCRIPTION SERVICES

The following current-awareness and literature-survey bibliographies are issued periodically by the Bureau:

Cryogenic Data Center Current Awareness Service. A literature survey issued biweekly. Annual subscription: domestic $25; foreign $30.

Liquefied Natural Gas. A literature survey issued quarterly. Annual subscription: $20.

Superconducting Devices and Materials. A literature survey issued quarterly. Annual subscription: $30. Please send subscription orders and remittances for the preceding bibliographic services to the National Bureau of Standards, Cryogenic Data Center (736) Boulder, CO 80303.

U.S. DEPARTMENT OF COMMERCE
National Bureau of Standards
Washington, D.C. 20234

OFFICIAL BUSINESS

Penalty for Private Use, $300

POSTAGE AND FEES PAID
U.S. DEPARTMENT OF COMMERCE
COM-215

SPECIAL FOURTH-CLASS RATE
BOOK